AERO-ASTRONAUTICS REPORT NO. 247

OPTIMAL TRAJECTORIES FOR AN AEROSPACE PLANE, PART 1: FORMULATION, RESULTS, AND ANALYSIS

by

A. MIELE, W. Y. LEE, AND G. D. WU

RICE UNIVERSITY

1990

AERO-ASTRONAUTICS REPORT NO. 247

OPTIMAL TRAJECTORIES FOR AN AEROSPACE PLANE, PART 1: FORMULATION, RESULTS, AND ANALYSIS

by

A. MIELE, W. Y. LEE, AND G. D. WU

RICE UNIVERSITY

1990

Optimal Trajectories for an Aerospace Plane, Part 1: Formulation, Results, and Analysis[1,2]

by

A. Miele[3], W. Y. Lee[4], and G. D. Wu[5]

---

[1]Portions of this material were presented by the senior author at the 1990 American Control Conference, San Diego, California, May 23-25, 1990.

[2]This research was supported by NASA Langley Research Center Grant No. NAG-1-1029 and by Texas Advanced Technology Program Grant No. TATP-003604020.

[3]Foyt Family Professor of Aerospace Sciences and Mathematical Sciences, Aero-Astronautics Group, Rice University, Houston, Texas.

[4]Post-Doctoral Fellow, Aero-Astronautics Group, Rice University, Houston, Texas.

[5]Graduate Student, Aero-Astronautics Group, Rice University, Houston, Texas.

Abstract. This paper is concerned with the optimization of the trajectories of an aerospace plane. This is a hypervelocity vehicle capable of achieving orbital speed, while taking off horizontally. The vehicle is propelled by four types of engines: turbojet engines for flight at subsonic speeds/low supersonic speeds; ramjet engines for flight at moderate supersonic speeds/low hypersonic speeds; scramjet engines for flight at hypersonic speeds; and rocket engines for flight at near-orbital speeds.

A single-stage-to-orbit (SSTO) configuration is considered, and the transition from low supersonic speeds to orbital speeds is studied under the following assumptions: the turbojet portion of the trajectory has been completed; the aerospace plane is controlled via the angle of attack $\alpha(t)$ and the power setting $\beta(t)$; the aerodynamic model is the generic hypersonic aerodynamics model example (GHAME). Concerning the engine model, three options are considered: (EM1) this is a ramjet/scramjet combination in which the scramjet specific impulse tends to a nearly-constant value at large Mach numbers; (EM2) this is a ramjet/scramjet combination in which the scramjet specific impulse decreases monotonically at large Mach numbers; (EM3) this is a ramjet/scramjet/rocket combination in which, owing to stagnation temperature limitations, the scramjet operates only at $M \leq 15$; at higher Mach numbers, the scramjet is shut off and the aerospace plane is driven only by the rocket engines.

Under the above assumptions, four optimization problems are solved using the sequential gradient-restoration algorithm for optimal control problems: (P1) minimization of the weight of fuel consumed; (P2) minimization of the peak dynamic pressure; (P3) minimization of the peak heating rate; and (P4) minimization of the peak tangential acceleration. The above optimization studies are carried out for different combinations of constraints, specifically: initial path inclination either free or given ($\gamma_0 = 0$); dynamic pressure either free or bounded ($q \leq 1500$ lbf/ft^2); tangential acceleration either free or bounded ($a_T \leq 3g_e$).

The preliminary conclusions are as follows:

(a) For an aerospace plane governed by GHAME + EM1, the SSTO mission requires a weight of fuel consumed equal to 34.3% of the initial weight.

(b) For an aerospace plane governed by GHAME + EM2, the SSTO mission requires a weight of fuel consumed equal to 44.3% of the initial weight.

(c) For an aerospace plane governed by GHAME + EM3, the SSTO mission requires a weight of fuel consumed equal to 60.7% of the initial weight.

(d) If one assumes that engine model EM2 is the one closer to reality, then the SSTO mission appears to be feasible. Obviously, its ability to deliver payloads can be improved via progress in the areas of aerodynamic properties and specific impulse properties.

(e) If one assumes that engine model EM3 is the one closer to reality, then the SSTO mission appears to be marginal, unless substantial progress is achieved in the areas of aerodynamic properties and specific impulse properties. Under this scenario, alternative consideration should be given to studying the feasibility of a two-stage-to-orbit (TSTO) mission.

Key Words. Flight mechanics, hypervelocity flight, atmospheric flight, optimal trajectories, aerospace plane, sequential gradient-restoration algorithm.

1. Introduction

The aerospace plane is a hypervelocity aircraft which must take off horizontally, achieve orbital speed, and then land horizontally. At this time, its configuration is not precisely known, but it can be assumed that the powerplant includes the combination of four types of engines: turbojet engines for flight at subsonic speeds/low supersonic speeds; ramjet engines for flight at moderate supersonic speeds/low hypersonic speeds; scramjet engines for flight at hypersonic speeds; and rocket engines for flight at near-orbital speeds.

In this paper, we refer to a single-stage-to-orbit (SSTO) configuration and we study the transition from low supersonic speeds to orbital speeds under the following assumptions: (i) the turbojet portion of the trajectory has been completed; (ii) the aerospace plane is controlled via the angle of attack $\alpha(t)$ and the power setting $\beta(t)$; (iii) the switch times from one powerplant to another are parameters being optimized.

Concerning the aerodynamics model, two configurations have been considered thus far in the aerospace plane literature: the generic hypersonic aerodynamics model example (GHAME) and the Langley accelerator model example (LAME). The first of these configurations (GHAME) is considered here.

Concerning the engine model, three options are considered: (EM1) this is a ramjet/scramjet combination in which the scramjet specific impulse tends to a nearly-constant value at

large Mach numbers; (EM2) this is a ramjet/scramjet combination in which the scramjet specific impulse decreases monotonically at large Mach numbers; (EM3) this is a ramjet/scramjet/rocket combination in which, owing to stagnation temperature limitations, the scramjet operates only at $M \leq M_*$; at higher Mach numbers, the scramjet is shut off and the aerospace plane is driven only by the rocket engines. Here, M_* is a threshold Mach number.

With the above understanding, we study four basic optimization problems: (P1) minimization of the weight of fuel consumed; (P2) minimization of the peak dynamic pressure; (P3) minimization of the peak heating rate; and (P4) minimization of the peak tangential acceleration. These optimization problems are solved by means of the sequential gradient-restoration algorithm (SGRA) for different combinations of constraints imposed on the initial path inclination γ_0, the dynamic pressure q, and the tangential acceleration a_T. Specifically, γ_0 can either be free or given ($\gamma_0 = 0$); q can either be free or bounded ($q \leq 1500$ lbf/ft^2); and a_T can either be free or bounded ($a_T \leq 3g_e$).

Previous studies of interest for the aerospace plane can be found in Refs. 1-19. References 1-3 contain basic concepts. References 4-8 deal with flight mechanics, hypervelocity flight, and propulsion systems. References 9-12 treat design problems, while Refs. 13-18 consider trajectory optimization and guidance. Concerning aerodynamics, two widely used configurations are the generic hypersonic aerodynamics model example (GHAME, Ref.19)

and the Langley accelerator model example (LAME). While GHAME has been used in Ref. 15, LAME has been considered in Ref. 16. Concerning the engine models, we note that EM1 has been considered in Ref. 15, while EM2 has been considered in Refs. 16-18. A model akin to EM3 has been considered in Ref. 10, albeit with a lower threshold Mach number than that considered in this paper.

Section 2 contains the notations, and Section 3 presents the system description. Sections 4-5 deal with the performance indexes and present a classification of the problems being studied. In Section 6, we present the results obtained on optimal trajectories for engine models EM1, EM2, EM3. Finally, the conclusions are given in Section 7.

2. Notations

Throughout this paper, the following notations are employed:

a = acceleration, ft/sec^2;

C_D = drag coefficient;

C_L = lift coefficient;

D = drag, lbf;

E = lift-to-drag ratio;

g = local acceleration of gravity, ft/sec^2;

g_e = sea-level acceleration of gravity, ft/sec^2;

h = altitude, ft;

I_{sp} = specific impulse, sec;

L = lift, lbf;

m = mass, lbf sec^2/ft;

M = Mach number;

q = dynamic pressure, lbf/ft^2;

Q = heating rate, BTU/ft^2sec;

r = radial distance from the center of the Earth, ft;

r_e = radius of the Earth, ft;

S = reference surface area, ft^2;

S_e = combustor cross-sectional area, ft^2;

t = dimensionless time;

T = thrust, lbf;

V = velocity, ft/sec;

$W = mg_e$ = sea-level weight, lbf;

x = distance along the Earth surface, ft;

α = angle of attack, rad;

β = power setting;

γ = path inclination, rad;

δ = inclination of the thrust with respect to the aircraft reference line, rad;

θ = running time, sec;

μ = Earth's gravitational constant, ft^3/sec^2;

ρ = air density, lbf sec^2/ft^4;

τ = final time, sec.

Subscripts (EM1 + EM2)

0 = beginning of ramjet phase/initial point;

1 = beginning of scramjet phase;

2 = end of scramjet phase/final point.

Subscripts (EM3)

0 = beginning of ramjet phase/initial point;

1 = beginning of scramjet phase;

2 = beginning of rocket phase;

3 = end of rocket phase/final point.

Superscript

$\cdot$ = derivative with respect to dimensionless time.

Acronyms

GHAME = general hypersonic aerodynamics model example;

LAME = Langley accelerator model example;

SGRA = sequential gradient-restoration algorithm;

SSTO = single-stage-to-orbit;

TSTO = two-stage-to-orbit.

3. System Description

We consider a single-stage-to-orbit (SSTO) aerospace plane, powered by the combination of turbojet/ramjet/scramjet/rocket engines. We employ the following hypotheses: (i) the turbojet portion of the trajectory has been completed; (ii) flight takes place in a vertical plane over a spherical Earth; (iii) the Earth's rotation is neglected; (iv) the gravitational field is central and obeys the inverse square law; (v) the aerospace plane is controlled via the angle of attack $\alpha(t)$ and the power setting $\beta(t)$.

3.1. Time Normalization. We denote with θ the actual time and with t the normalized time. The normalization is done in such a way that the normalized time duration of each segment of the trajectory is one. Hence, the transformation relations are as follows:

$$\theta = \tau_1 t, \qquad 0 \leq t \leq 1 \quad \text{(ramjet)}, \tag{1a}$$

$$\theta = \tau_1 + \tau_2 (t-1), \qquad 1 \leq t \leq 2 \quad \text{(scramjet)}, \tag{1b}$$

$$\theta = \tau_1 + \tau_2 + \tau_3 (t-2), \qquad 2 \leq t \leq 3 \quad \text{(rocket)}, \tag{1c}$$

with the implication that

$$\dot{\theta} = \tau_1, \qquad 0 \leq t \leq 1 \quad \text{(ramjet)}, \tag{2a}$$

$$\dot{\theta} = \tau_2, \qquad 1 \leq t \leq 2 \quad \text{(scramjet)}, \tag{2b}$$

$$\dot{\theta} = \tau_3, \qquad 2 \leq t \leq 3 \quad \text{(rocket)}, \tag{2c}$$

and that

$$\theta_0 = 0, \tag{3a}$$

$$\theta_1 = \tau_1, \tag{3b}$$

$$\theta_2 = \tau_1 + \tau_2, \tag{3c}$$

$$\theta_3 = \tau_1 + \tau_2 + \tau_3. \tag{3d}$$

Note that θ_2 is the final time for engine models EM1, EM2 and that θ_3 is the final time for engine model EM3.

3.2. Differential System. With the above assumptions and upon normalizing the time duration of each segment of the trajectory to unity, the motion of the aerospace plane is described by the following differential system:

$$\dot{x} = \tau[(r_e/r)V\cos\gamma], \tag{4a}$$

$$\dot{h} = \tau[V\sin\gamma], \tag{4b}$$

$$\dot{V} = \tau[(Tg_e/W)\cos(\alpha + \delta) - Dg_e/W - g\sin\gamma], \tag{4c}$$

$$\dot{\gamma} = \tau[(Tg_e/WV)\sin(\alpha + \delta) + Lg_e/WV + (V/r - g/V)\cos\gamma], \tag{4d}$$

$$\dot{W} = \tau[-T/I_{sp}]. \tag{4e}$$

Here, the dot denotes derivative with respect to the normalized time and the flight duration τ takes the following values: $\tau = \tau_1$ for the ramjet segment, $\tau = \tau_2$ for the scramjet segment, and $\tau = \tau_3$ for the rocket segment of the trajectory.

In the above system, the following functional relations hold:

$$r = r_e + h, \tag{5a}$$

$$g = \mu/r^2 = \mu/(r_e + h)^2, \tag{5b}$$

where $\mu = g_e r_e^2$ denotes the Earth's gravitational constant. The weight $W = mg_e$ appearing in Eqs. (4) is the so-called sea-level weight, which is based on the sea-level acceleration of gravity g_e. Such weight differs from the local weight mg, which is based on the local acceleration of gravity g.

3.3. Aerodynamic Data. The drag and the lift are given by

$$D = (1/2)C_D \rho S V^2, \tag{6a}$$

$$L = (1/2)C_L \rho S V^2, \tag{6b}$$

with $\rho = \rho(h)$. Generally speaking, the aerodynamic coefficients C_D, C_L depend on the angle of attack α, the Mach number M, and the Reynolds number Re. If the dependence on the Reynolds number is disregarded, the aerodynamic coefficients take the form

$$C_D = C_D(\alpha, M), \tag{7a}$$

$$C_L = C_L(\alpha, M), \tag{7b}$$

with the implication that the lift-to-drag ratio $E = L/D = C_L/C_D$ is a function of the form

$$E = E(\alpha, M). \tag{7c}$$

The functions (7) are plotted in Fig. 1 with reference to the generic hypersonic aerodynamics model example (GHAME).

For computational purposes, it is convenient to approximate the aerodynamic coefficients with polynomial relations of the type

$$C_D = A_0(M) + A_1(M)\alpha + A_2(M)\alpha^2, \tag{8a}$$

$$C_L = B_0(M) + B_1(M)\alpha + B_2(M)\alpha^2, \tag{8b}$$

with the implication that

$$E = [B_0(M) + B_1(M)\alpha + B_2(M)\alpha^2]/[A_0(M) + A_1(M)\alpha + A_2(M)\alpha^2]. \tag{8c}$$

The coefficients $A_i(M)$, $B_i(M)$ are computed by means of a least square fit of the available GHAME data at various Mach numbers and angles of attack.

3.4. Engine Data. For the ramjet engines, the following simplified representation is assumed for the thrust and the specific impulse:

$$T = \beta T_*(M)\rho/\rho_*, \tag{9a}$$

$$I_{sp} = I_{sp*}(M), \tag{9b}$$

with the implication that the fuel rate (weight of fuel consumed per unit time) is given by

$$T/I_{sp} = \beta[T_*(M)/I_{sp*}(M)]\rho/\rho*. \tag{9c}$$

Here, ρ_* is a reference density (density at the reference altitude $h_* = 100$ kft), $T_*(M)$ is a reference thrust (thrust for $\beta = 1$ and $h = h_*$), and $I_{sp*}(M)$ is a reference specific impulse (specific impulse for $\beta = 1$ and $h = h_*$). While the thrust is assumed to depend on the power setting, the altitude, and the Mach number,

the specific impulse is assumed to depend only on the Mach number; the dependence of the specific impulse on the power setting and the altitude is disregarded in line with the feasibility character of the present study. For the same reason, the dependence of the thrust and the specific impulse on the angle of attack, relevant to a precision study, is disregarded within the bounds of the present feasibility study.

For the scramjet engines, the representation (9) is retained. However, the reference thrust $T_*(M)$ and the reference specific impulse $I_{sp*}(M)$ are now described by different functions.

For the rocket engines, the following simplified relations are assumed:

$$T = \beta T_*, \tag{10a}$$

$$I_{sp} = I_{sp*}, \tag{10b}$$

with the implication that the fuel rate is given by

$$T/I_{sp} = \beta(T_*/I_{sp*}). \tag{10c}$$

Here, T_* is a reference thrust (thrust for $\beta = 1$) and I_{sp*} is a reference specific impulse (specific impulse for $\beta = 1$). Both T_* and I_{sp*} are assumed to be constant. This means that the weak dependence of these quantities on the altitude is disregarded.

In this paper, three engine models are considered:

(EM1) This is a ramjet/scramjet combination in which the scramjet specific impulse tends to a nearly-constant value at

large Mach numbers;see Ref. 15. For this combination, the functions (9) are shown in Fig. 2 (ramjet) and Fig. 3 (scramjet) under the assumption that the combustor cross-sectional area is $S_e = 400\ ft^2$.

(EM2) This is a ramjet/scramjet combination in which the scramjet specific impulse decreases monotonically at large Mach numbers; see Refs. 16-18. For this combination, the functions (9) are shown in Fig. 2 (ramjet) and Fig. 4 (scramjet) under the assumption that the combustor cross-section area is $S_e = 400\ ft^2$.

(EM3) This is a ramjet/scramjet/rocket combination in which, owing to stagnation temperature limitations, the scramjet operates only at $M \leq 15$; at higher Mach numbers, the scramjet is shut off and the aerospace plane is driven only by the rocket engines. For this combination, the functions (9) are shown in Fig. 2 (ramjet) and Fig. 5 (scramjet, $M \leq 15$) under the assumption that the combustor cross-sectional area is $S_e = 400\ ft^2$; the functions (10) are shown in Fig. 6 (rocket, $M \geq 15$) under the assumption that the reference thrust (hence, the maximum thrust) is $T_* = 189200$ lbf.

3.5. Control Inequality Constraints. To obtain realistic solutions, the presence of upper and lower bounds on the angle of attack and the power setting is necessary. Therefore, the two-sided inequality constraints

$$\alpha_\ell \leq \alpha \leq \alpha_u, \tag{11a}$$

$$\beta_\ell \leq \beta \leq \beta_u \tag{11b}$$

must be satisfied everywhere along the interval of integration.

The inequality constraints (11) can be converted into equality constraints by means of trigonometric transformations of the type

$$\alpha = (1/2)(\alpha_\ell + \alpha_u) + (1/2)(\alpha_u - \alpha_\ell)\sin u, \tag{12a}$$

$$\beta = (1/2)(\beta_\ell + \beta_u) + (1/2)(\beta_u - \beta_\ell)\sin w. \tag{12b}$$

Therefore, the angle of attack $\alpha(t)$ is replaced with the auxiliary control $u(t)$, while the power setting $\beta(t)$ is replaced with the auxiliary control $w(t)$. After a solution is found for the auxiliary controls, then the original controls are computed with (12).

For the GHAME configuration, the bounds (11a) are given by

$$\alpha_\ell = -2.0 \text{ deg}, \qquad \alpha_u = 12.0 \text{ deg}. \tag{13a}$$

These bounds are dictated solely by the availability of data. For the engine models EM1, EM2, EM3, the bounds (11b) are given by

$$\beta_\ell = 0, \qquad \beta_u = 1. \tag{13b}$$

3.6. Derived Quantities. After a solution of Eqs. (4) is available, certain derived quantities can be computed. The more relevant ones are listed below:

(i) the dynamic pressure

$$q = (1/2)\rho V^2; \tag{14a}$$

(ii) the heating rate

$$Q = C\sqrt{(\rho/\rho_*)}(V/V_*)^{3.07}; \tag{14b}$$

here, ρ_* is a reference density (density at $h_* = 100$ kft) and V_* is a reference velocity ($V_* = 10$ kft/sec); under the assumption that the nose radius is $r_n = 1.0$ ft, the constant C has the value $C = 101.92$ BTU/ft^{2}sec;

(iii) the tangential acceleration

$$a_T = (Tg_e/W)\cos(\alpha + \delta) - Dg_e/W - g\sin\gamma; \tag{14c}$$

(iv) the normal acceleration

$$a_N = (Tg_e/W)\sin(\alpha + \delta) + Lg_e/W + (V^2/r - g)\cos\gamma; \tag{14d}$$

(v) the total acceleration

$$a = \sqrt{(a_T^2 + a_N^2)}. \tag{14e}$$

3.7. Supplementary Bounds. In addition to the control inequality constraints (11), supplementary bounds can be imposed on the quantities (14). For instance, a bound of the form [see (14a)]

$$q \leq q_u = 1500 \text{ lbf/ft}^2 \tag{15a}$$

is a state constraint, while a bound of the form [see (14c)]

$$a_T \leq a_{Tu} = 3g_e \tag{15b}$$

is a state/control constraint.

The simplest way to account for the bounds (15) is by means of penalization techniques. The functional being minimized (see Section 4) is augmented by a penalization functional with integrand

$$C_1(q - q_u)^n + C_2(a_T - a_{Tu})^n, \tag{15c}$$

where C_1, C_2 are constants and n is a suitable integer. The value of the first constant is $C_1 = 0$ if (15a) is satisfied and $C_1 > 0$ if (15a) is violated; the value of the second constant is $C_2 = 0$ if (15b) is satisfied and $C_2 > 0$ if (15b) is violated; the desirable value of the integer is n = 3, since this ensures the continuity of the first and second derivatives of the integrand of the penalization functional at points located on the constraint boundaries.

3.8. Boundary Conditions. For engine models EM1, EM2, EM3, the dimensionless time t = 0 marks the end of the turbojet phase, the beginning of the ramjet phase, as well as the initial time. At t = 0, we assume that

$$x_0 = 0 \text{ ft}, \tag{16a}$$

$$h_0 = 42004 \text{ ft} = 12.8 \text{ km}, \tag{16b}$$

$$V_0 = 1936 \text{ ft/sec}, \tag{16c}$$

$$\gamma_0 = \text{free or } \gamma_0 = 0.0 \text{ deg}, \tag{16d}$$

$$W_0 = 290000 \text{ lbf}, \tag{16e}$$

with the implication that

$$M_0 = 2, \tag{16f}$$

$$q_0 = 1000 \text{ lbf/ft}^2. \tag{16g}$$

For engine models EM1, EM2, EM3, the dimensionless time $t = 1$ marks the end of the ramjet phase and the beginning of the scramjet phase. At $t = 1$, the continuity of all the state variables is required.

For engine models EM1 and EM2, the dimensionless time $t = 2$ marks the end of the scramjet phase as well as final time. At $t = 2$, we assume that

$$x_2 = \text{free}, \tag{17a}$$

$$h_2 = 262467 \text{ ft} = 80.0 \text{ km}, \tag{17b}$$

$$V_2 = 25792 \text{ ft/sec}, \tag{17c}$$

$$\gamma_2 = 0.0 \text{ deg}, \tag{17d}$$

$$W_2 = \text{free}, \tag{17e}$$

with the implication that

$$M_2 = 27.8, \tag{17f}$$

$$q_2 = 11.9 \text{ lbf/ft}^2, \tag{17g}$$

and that orbital speed is achieved.

For engine model EM3, the dimensionless time $t = 2$ marks the end of the scramjet phase and the beginning of the rocket phase. At $t = 2$, we assume that

$$M_2 = 15. \tag{18}$$

In addition, we require the continuity of all the state variables.

For engine model EM3, the dimensionless time t = 3 marks the end of the rocket phase as well as the final time. At t = 3, we assume that

$$x_3 = \text{free}, \tag{19a}$$

$$h_3 = 262467 \text{ ft} = 80.0 \text{ km}, \tag{19b}$$

$$V_3 = 25792 \text{ ft/sec}, \tag{19c}$$

$$\gamma_3 = 0.0 \text{ deg}, \tag{19d}$$

$$W_3 = \text{free}, \tag{19e}$$

with the implication that

$$M_3 = 27.8, \tag{19f}$$

$$q_3 = 11.9 \text{ lbf/ft}^2, \tag{19g}$$

and that orbital speed has been achieved.

3.9. Summary. The relations governing the motion of the aerospace plane include: the differential system (4); the control inequality constraints (11), converted into control equality constraints by means of the trigonometric transformations (12);the possible presence of the supplementary bounds (15), accounted via penalization techniques; the boundary conditions (16)-(17) for engine models EM1, EM2; and the boundary conditions (16), (18), (19) for engine model EM3.

In this formulation, the independent variable is the time t, which varies in the range $0 \leq t \leq 2$ for engine models EM1, EM2 and in the range $0 \leq t \leq 3$ for engine model EM3. The dependent

variables include five state variables [x(t), h(t), V(t), γ(t), W(t)], two control variables [u(t), w(t)], plus two parameters [τ_1, τ_2] for engine models EM1, EM2 and three parameters [τ_1, τ_2, τ_3] for engine model EM3. After a solution is found for the auxiliary control variables, the original control variables [α(t), β(t)] are recovered via the trigonometric transformations (12).

3.10. Experimental Data. The following data are used in the numerical experiments on optimal trajectories.

Spaceplane. For the aerospace plane, the initial weight (weight at the end of the turbojet phase) is W_0 = 290000 lbf; the reference surface area (wing area) is S = 6000 ft^2; the aerodynamic data for the GHAME configuration are given in Fig. 1; the angle of attack is subject to the inequality $-2.0 \leq \alpha \leq 12.0$ deg.

Engines. The data for engine models EM1, EM2, EM3 are given in Figs. 2-6. For all models, the combustor cross-sectional area of both the ramjet and the scramjet is S_e = 400 ft^2. For engine model EM3, the maximum rocket thrust is T_* = 189200 lbf and the rocket specific impulse is I_{sp} = 444 sec. The inclination of the thrust with respect to the aircraft reference line is δ = 0.0 deg; the power setting is subject to the inequality $0 \leq \beta \leq 1$.

Physical Constants. The radius of the Earth is assumed to be r_e = 0.2093E+08 ft = 6378 km. The Earth's gravitational constant is μ = 0.1409E+17 ft^3/sec^2. The sea-level acceleration of gravity is g_e = 32.20 ft/sec^2.

Atmospheric Model. The atmospheric model used is the US Standard Atmosphere, 1976 (Ref. 20). In this model, the values of the density are tabulated at discrete altitudes. For intermediate

altitudes, the density is computed by assuming an exponential fit for the function $\rho(h)$. This is equivalent to assuming that the atmosphere behaves isothermally between any two contiguous altitudes tabulated in Ref. 20.

4. Performance Indexes

Subject to the previous constraints, different optimization problems can be formulated, depending on the performance index being considered. The resulting optimal control problems are either of the Bolza type or of the Chebyshev type.

Problem (P1). Minimum Fuel Weight. It is required to minimize the weight of fuel consumed. Here, the performance index is given by

$$I = W_0 - W_2 \quad (EM1, EM2), \tag{20a}$$

or

$$I = W_0 - W_3 \quad (EM3). \tag{20b}$$

Problem (P2). Minimum Peak Dynamic Pressure. It is required to minimize the peak value of the dynamic pressure. Here, the performance index is given by

$$I = \max_t(q), \tag{21a}$$

where the dynamic pressure is given by [see (14a)]

$$q = (1/2)\rho V^2. \tag{21b}$$

This problem can be reformulated as that of minimizing the integral performance index

$$J = \int_0^2 q^n dt \quad (EM1, EM2), \tag{21c}$$

or

$$J = \int_0^3 q^n dt \qquad \text{(EM3)}, \tag{21d}$$

with n = 8.

Problem (P3). Minimum Peak Heating Rate. It is required to minimize the peak value of the heating rate at a particular point of the aerospace plane, for instance, the stagnation point. Here, the performance index is given by

$$I = \max_t (Q), \tag{22a}$$

where the heating rate is given by [see (14b)]

$$Q = C\sqrt{(\rho/\rho_*)}(V/V_*)^{3.07}. \tag{22b}$$

This problem can be reformulated as that of minimizing the integral performance index

$$J = \int_0^2 Q^n dt \qquad \text{(EM1, EM2)}, \tag{22c}$$

or

$$J = \int_0^3 Q^n dt \qquad \text{(EM3)}, \tag{22d}$$

with n = 8.

Problem (P4). Minimum Peak Tangential Acceleration. It is required to minimize the peak value of the tangential acceleration. Here, the performance index is given by

$$I = \max_t (a_T), \tag{23a}$$

where the tangential acceleration is given by [see (14c)]

$$a_T = (Tg_e/W)\cos(\alpha + \delta) - Dg_e/W - g\sin\gamma. \tag{23b}$$

This problem can be reformulated as that of minimizing the integral performance index

$$J = \int_0^2 a_T^n dt \qquad (EM1, EM2), \tag{23c}$$

or

$$J = \int_0^3 a_T^n dt \qquad (EM3), \tag{23d}$$

with $n = 8$.

5. Problem Classification

In the analyses which follow, the initial path inclination γ_0 is either free or given (γ_0 = 0.0 deg); the dynamic pressure q is either free or bounded ($q \leq q_u$); and the tangential acceleration a_T is either free or bounded ($a_T \leq a_{Tu}$). Depending on the combination of constraints being considered, we have the following types of problems:

$$\text{(A)} \quad \gamma_0 = \text{free}, \qquad q = \text{free}, \qquad a_T = \text{free}, \tag{24a}$$

$$\text{(B)} \quad \gamma_0 = \text{free}, \qquad q \leq q_u, \qquad a_T \leq a_{Tu}, \tag{24b}$$

$$\text{(C)} \quad \gamma_0 = 0.0 \text{ deg}, \qquad q = \text{free}, \qquad a_T = \text{free}, \tag{24c}$$

$$\text{(D)} \quad \gamma_0 = 0.0 \text{ deg}, \qquad q \leq q_u, \qquad a_T \leq a_{Tu}, \tag{24d}$$

with

$$q_u = 1500 \text{ lbf/ft}^2, \quad a_{Tu} = 3g_e. \tag{25}$$

Note that a peak heating rate bound,

$$Q \leq Q_u, \tag{26a}$$

with

$$Q_u = 150 \text{ BTU/ft}^2\text{sec}, \tag{26b}$$

is not imposed because it can be satisfied or nearly satisfied indirectly if the dynamic pressure bound is satisfied.

The ensuing terminology is self-explanatory for the minimum fuel weight problem:

Problem (P1A) is Problem (P1), s.t. conditions (A),

Problem (P1B) is Problem (P1), s.t. conditions (B),

Problem (P1C) is Problem (P1), s.t. conditions (C),

Problem (P1D) is Problem (P1), s.t. conditions (D).

A similar terminology is employed for the problems of minimizing the peak dynamic pressure, the peak heating rate, and the peak tangential acceleration.

To sum up, for a given aerodynamic configuration and a given engine model, there are 16 optimization problems to be solved. Since there are three engine models, this leads to a total of 48 optimization problems to be solved.

6. Numerical Results

Numerical solutions for the optimization problems formulated in Sections 4-5 were obtained by means of the sequential gradient-restoration algorithm (SGRA, Refs. 21-22). We recall that SGRA is a first-order algorithm which generates a sequence of feasible solutions, each characterized by a lower value of the performance index being considered.

While SGRA is available in both primal form (PSGRA) and dual form (DSGRA), the primal form is better suited for hypervelocity flight problems; hence, it is employed here. A cross section of the solutions obtained is presented in Tables 1-3. For more details on the solutions, see Ref. 23.

6.1. Unconstrained Solutions. First, constraints of Type (A) were considered [see (24a)], meaning that γ_0 is free, the dynamic pressure q is unconstrained, and the tangential acceleration a_T is unconstrained. For constraints of Type (A) and for engine model EM1, SGRA was employed to minimize each of the performance indexes of Section 4. Summary results are shown in Table 1, which lists the values of the weight of fuel consumed, the peak dynamic pressure, the peak heating rate, and the peak tangential acceleration for Problems (P1A), (P2A), (P3A), (P4A). Table 1 also lists the initial path inclination γ_0, the time duration of each segment of the trajectory (τ_1, τ_2), and the final time $\theta_f = \theta_2$.

In interpreting the results of Table 1, we stress the following concept: even though these results have been obtained disregarding the presence of constraints on γ_0, q, Q, a_T, these

results are acceptable from an engineering point of view only if γ_0, max(q), max(Q), max(a_T) are in a suitable range. Specifically, γ_0 should be relatively small, otherwise an intolerable burden is imposed on the turbojet segment of the trajectory; max(q) should be less than 1500 lb/ft^2; max(Q) should be less than 150 BTU/ft^{2}sec; and max(a_T) should be less than $3g_e$.

Inspection of Table 1 shows that solution (P1A) is not acceptable mainly because the values of γ_0 and max(a_T) are excessive; solution (P2A) is not acceptable because the values of γ_0 and max(a_T) are excessive; solution (P3A) is not acceptable because the values of γ_0 and max(a_T) are excessive; and solution (P4A) is not acceptable because the values of γ_0, max(q), max(Q) are excessive. In addition, for solution (P4A), the weight of fuel consumed is too large with respect to that of solution (P1A).

6.2. Constrained Solutions. Next, Problem (P1) is considered [see (20)], meaning that the weight of fuel consumed is being minimized. For Problem (P1) and for engine model EM1, SGRA was employed to obtain minimum fuel solutions for each of the constraint combinations (24). Summary results are shown in Table 2, which lists the values of the weight of fuel consumed, the peak dynamic pressure, the peak heating rate, and the peak tangential acceleration for Problems (P1A), (P1B), (P1C), (P1D). Table 2 also lists the initial path inclination γ_0, the time duration of each segment of the trajectory (τ_1, τ_2), and the final time $\theta_f = \theta_2$.

Inspection of Table 2 shows that solution (P1A) is not acceptable mainly because the values of γ_0 and max(a_T)

are excessive; solution (P1B) is not acceptable because the value of γ_0 is excessive; solution (P1C) is not acceptable because the values of max(q), max(Q), max(a_T) are excessive. The only acceptable solution is solution (P1D), albeit with a 1.7% increase in fuel weight with respect to that of solution (P1A).

6.3. Effect of the Engine Model. Thus far, the only acceptable solution is (P1D), which is obtained by minimizing the weight of fuel consumed [Problem (P1)] in conjunction with constraints of Type (D). Therefore, we consider now Problem (P1D) for different engine models (EM1, EM2, EM3).

We recall that engine model EM1 is a ramjet/scramjet combination with scramjet specific impulse tending to a nearly-constant value at large Mach numbers; engine model EM2 is a ramjet/scramjet combination with scramjet specific impulse decreasing monotonically at large Mach numbers; engine model EM3 is a ramjet/scramjet/rocket combination in which the scramjet operates only at $M \leq 15$; at higher Mach numbers, the scramjet is shut off and the aerospace plane is driven only by the rocket engines.

Summary results are shown in Table 3, which lists the values of the weight of fuel consumed, the peak dynamic pressure, the peak heating rate, and the peak tangential acceleration for Problem (P1D) and engine models EM1, EM2, EM3. Table 3 also lists the initial path inclination γ_0, the time duration of each segment of the trajectory [(τ_1, τ_2) for engine models EM1, EM2 and (τ_1, τ_2, τ_3) for engine model EM3], and the final time [$\theta_f = \theta_2$ for engine models EM1, EM2 and $\theta_f = \theta_3$ for engine model EM3].

Inspection of Table 3 shows that the constraints on max(q), max(Q), max(a_T) are now satisfied or nearly satisfied for all engine models. Note that γ_0 = 0.0 deg for all engine models. In percentage of the initial weight, the weight of fuel consumed is 34.3% for engine model EM1, 44.3% for engine model EM2, and 60.7% for engine model EM3.

Note that the above results exclude the turbojet segment of the trajectory. If one assumes that the weight of fuel consumed in the turbojet phase is 5% of the take-off weight, one concludes that, in percentage of the take-off weight, the weight of fuel consumed is 37.6% for engine model EM1, 47.1% for engine model EM2, and 62.7% for engine model EM3.

6.4. Remark. For Problem (P1D) solved in conjunction with engine model EM3, one additional simplification was used. The rocket portion of the trajectory, corresponding to $M \geq 15$, was optimized with the following provision: while the angle of attack $\alpha(t)$ is treated as a control, the power setting $\beta(t)$ is treated as a parameter, which means that $\dot{\beta}(t) = 0$ for $M \geq 15$.

7. Conclusions

This paper is concerned with optimizing the trajectories of an aerospace plane. A single-stage-to-orbit (SSTO) configuration is considered, and the transition from low supersonic speeds to orbital speeds is studied under the following assumptions: the turbojet portion of the trajectory has been completed; the aerospace plane is controlled via the angle of attack $\alpha(t)$ and the power setting $\beta(t)$; the aerodynamic model is the generic hypersonic aerodynamics model example (GHAME). Concerning the engine model, three options are considered: (EM1) this is a ramjet/scramjet combination in which the scramjet specific impulse tends to a nearly-constant value at large Mach numbers; (EM2) this is a ramjet/scramjet combination in which the scramjet specific impulse decreases monotonically at large Mach numbers; (EM3) this is a ramjet/scramjet/rocket combination in which, owing to stagnation temperature limitations, the scramjet operates only at $M \leq 15$; at higher Mach numbers, the scramjet is shut off and the aerospace plane is driven only by the rocket engines.

Under the above assumptions, four optimization problems are solved using the sequential gradient-restoration algorithm for optimal control problems: (P1) minimization of the weight of fuel consumed; (P2) minimization of the peak dynamic pressure; (P3) minimization of the peak heating rate; and (P4) minimization of the peak tangential acceleration.

The above optimization studies are carried out for different combinations of constraints, specifically: initial path inclination either free or given ($\gamma_0 = 0$); dynamic pressure either free or bounded ($q \leq 1500$ lbf/ft^2); tangential acceleration either free or bounded ($a_T \leq 3g_e$). A peak heating rate bound ($Q \leq 150$ BTU/ft^{2}sec) is not imposed because it can be nearly satisfied indirectly if the dynamic pressure bound is satisfied.

The effect of the performance index, the constraint type, and the engine model on the solutions is studied. From an engineering point of view, the most useful solutions are those which minimize the fuel weight, while satisfying the constraints $\gamma_0 = 0$, $q \leq 1500$ lbf/ft^2, $Q \leq 150$ BTU/ft^{2}sec, $a_T \leq 3g_e$.

The preliminary conclusions are as follows:

(a) For an aerospace plane governed by GHAME + EM1, the SSTO mission requires a weight of fuel consumed equal to 34.3% of the weight at the beginning of the ramjet phase, equivalent to 37.6% of the take-off weight if one includes the turbojet phase.

(b) For an aerospace plane governed by GHAME + EM2, the SSTO mission requires a weight of fuel consumed equal to 44.3% of the weight at the beginning of the ramjet phase, equivalent to 47.1% of the take-off weight if one includes the turbojet phase.

(c) For an aerospace plane governed by GHAME + EM3, the SSTO mission requires a weight of fuel consumed equal to 60.7% of the weight at the beginning of the ramjet phase, equivalent to 62.7% of the take-off weight if one includes the turbojet phase.

(d) If one assumes that engine model EM2 is the one closer to reality, then the SSTO mission appears to be feasible. Obviously, its ability to deliver payloads can be improved via progress in the areas of aerodynamic properties and specific impulse properties.

(e) If one assumes that engine model EM3 is the one closer to reality, then the SSTO mission appears to be marginal, unless substantial progress is achieved in the areas of aerodynamic properties and specific impulse properties. Under this scenario, alternative consideration should be given to studying the feasibility of a two-stage-to-orbit mission (TSTO mission).

References

1. KLUGER, J., Space Plane, Discover, Vol. 10, No. 11, pp. 81-84, 1989.

2. WILLIAMS, R. M., National Aerospace Plane: Technology for America's Future, Aerospace America, Vol. 24, No. 11, pp. 18-22, 1986.

3. PILAND, W. M., Technology Challenges for the National Aerospace Plane, Paper No. IAF-87-205, 38th Congress of the International Astronautical Federation, Brighton, England, 1987.

4. MIELE, A., Flight Mechanics, Vol. 1: Theory of Flight Paths, Addison-Wesley Publishing Company, Reading, Massachusetts, 1962.

5. VINH, N. X., BUSEMANN, A., and CULP, R. D., Hypersonic and Planetary Entry Flight Mechanics, University of Michigan Press, Ann Arbor, Michigan, 1980.

6. MIELE, A., Editor, Special Issue on Hypervelocity Flight, Journal of the Astronautical Sciences, Vol. 36, Nos. 1-2, pp. 1-197, 1988.

7. KERREBROCK, J. L., Aircraft Engines and Gas Turbines, MIT Press, Cambridge, Massachusetts, 1977.

8. LOH, W. H. T., Editor, Jet, Rocket, Nuclear, Ion and Electric Propulsion: Theory and Design, Springer-Verlag, New York, New York, 1968.

9. OLDS, J. R., A Conceptual Design for a Single-Stage-to-Orbit Space Station Service Vehicle, Paper No. IAF-ST-87-07, 38th Congress of the International Astronautical Federation, Brighton, England, 1987.

10. MARTIN, J. A., An Evaluation of Composite Propulsion for Single-Stage-to-Orbit Vehicles Designed for Horizontal Take-Off, NASA Technical Memorandum No. X-3554, 1977.

11. LEPSCH, R. A., Jr., STANLEY, D. O., CRUZ, C. I., and MORRIS, S. J., Jr., Utilizing Air-Turborocket and Rocket Propulsion for a Single-Stage-to-Orbit Vehicle, Paper No. AIAA-90-0295, 28th Aerospace Sciences Meeting, Reno, Nevada, 1990.

12. SCHOETTLE, U. M., Performance Analysis of Rocket-Ramjet Propelled SSTO Vehicles, Paper No. IAF-85-133, 36th Congress of the International Astronautical Federation, Stockholm, Sweden, 1985.

13. DELATTRE, P., and POTHIER, S., Airbreathing TSTO Trajectory Optimization, Paper No. IAF-89-360, 40th Congress of the International Astronautical Federation, Malaga, Spain, 1989.

14. LANDIECH, P., AUMASSON, C., and DROZ, J., Airbreathing Launchers Trajectory Optimization, Paper No. IAF-89-359, 40th Congress of the International Astronautical Federation, Malaga, Spain, 1989.

15. VAN BUREN, M. A., and MEASE, K. D., Minimum-Fuel Ascent to Orbit Using Air-Breathing Propulsion, Proceedings of the 1989 American Control Conference, Pittsburgh, Pennsylvania, pp. 2482-2488, 1989.

16. VAN BUREN, M. A., and MEASE, K. D., Aerospace Plane Guidance Using Geometric Control Theory, Proceedings of the 1990 American Control Conference, San Diego, California, pp. 1829-1838, 1990.

17. CORBAN, J. E., CALISE, A. J., and FLANDRO, G. A., A Real-Time Guidance Algorithm for Aerospace Plane Optimal Ascent to Low Earth Orbit, Proceedings of the 1989 American Control Conference, Pittsburgh, Pennsylvania, pp. 2475-2481, 1989.

18. CALISE, A. J., CORBAN, J. E., and FLANDRO, G. A., Trajectory Optimization and Guidance Law Development for National Aerospace Plane Applications, Proceedings of the 1988 American Control Conference, Atlanta, Georgia, pp. 1406-1411, 1988.

19. BOWERS, A. H., and ILIFF, K. W., A Generic Hypersonic Aerodynamic Model Example (GHAME) for Computer Simulation, NASA Technical Memorandum No. xxxx, 1988.

20. NOAA, NASA, and USAF, US Standard Atmosphere, 1976, US Government Printing Office, Washington, DC, 1976.

21. MIELE, A., and WANG, T., Primal-Dual Properties of Sequential Gradient-Restoration Algorithms for Optimal Control Problems, Part 1, Basic Problem, Integral Methods in Science and Engineering, Edited by F. R. Payne et al, Hemisphere Publishing Corporation, Washington, DC, pp. 577-607, 1986.

22. MIELE, A., and WANG, T., Primal-Dual Properties of Sequential Gradient-Restoration Algorithms for Optimal Control Problems, Part 2, General Problem, Journal of Mathematical Analysis and Applications, Vol. 119, Nos. 1-2, pp. 21-54, 1986.

23. MIELE, A., LEE, W. Y., and WU, G. D., Optimal Trajectories for an Aerospace Plane, Part 2: Data, Tables, and Graphs, Rice University, Aero-Astronautics Report No. 248, 1990.

Table 1. Unconstrained solutions, engine model EM1, various performance indexes, constraints of Type (A).

Quantity	Problem				Units
	(P1A)	(P2A)	(P3A)	(P4A)	
$(W_0-W_f)/W_0$	0.337	0.347	0.357	0.550	-
max(q)	1540	999	1157	3751	lbf/ft^2
max(Q)	165	161	98	495	BTU/ft^2sec
$max(a_T)/g_e$	9.1	5.2	4.0	1.1	-
γ_0	42.0	50.0	40.4	38.3	deg
τ_1	34	54	48	144	sec
τ_2	409	475	731	704	sec
θ_f	443	529	779	848	sec

$W_f = W_2$ and $\theta_f = \theta_2$ for engine model EM1.

Table 2. Constrained solutions, engine model EM1, minimum fuel weight, various constraint combinations.

Quantity	Problem				Units
	(P1A)	(P1B)	(P1C)	(P1D)	
$(W_0-W_f)/W_0$	0.337	0.340	0.339	0.343	-
max(q)	1540	1112	1765	1500	lbf/ft^2
max(Q)	165	148	200	153	BTU/ft^2sec
$max(a_T)/g_e$	9.1	3.0	13.7	3.0	-
γ_0	42.0	39.4	0.0	0.0	deg
τ_1	34	55	34	55	sec
τ_2	409	498	335	487	sec
θ_f	443	553	369	542	sec

$W_f = W_2$ and $\theta_f = \theta_2$ for engine model EM1.

Table 3. Effect of the engine model, Problem (P1D), minimum fuel weight, constraints of Type (D).

Quantity	Engine model			Units
	EM1	EM2	EM3	
$(W_0-W_f)/W_0$	0.343	0.443	0.607	-
max(q)	1500	1425	1500	lbf/ft^2
max(Q)	153	157	110	BTU/ft^2sec
$max(a_T)/g_e$	3.0	3.0	3.0	-
γ_0	0.0	0.0	0.0	deg
τ_1	55	44	57	sec
τ_2	487	472	97	sec
τ_3	-	-	277	sec
θ_f	542	517	431	sec

$W_f = W_2$ and $\theta_f = \theta_2$ for engine models EM1, EM2.

$W_f = W_3$ and $\theta_f = \theta_3$ for engine model EM3.

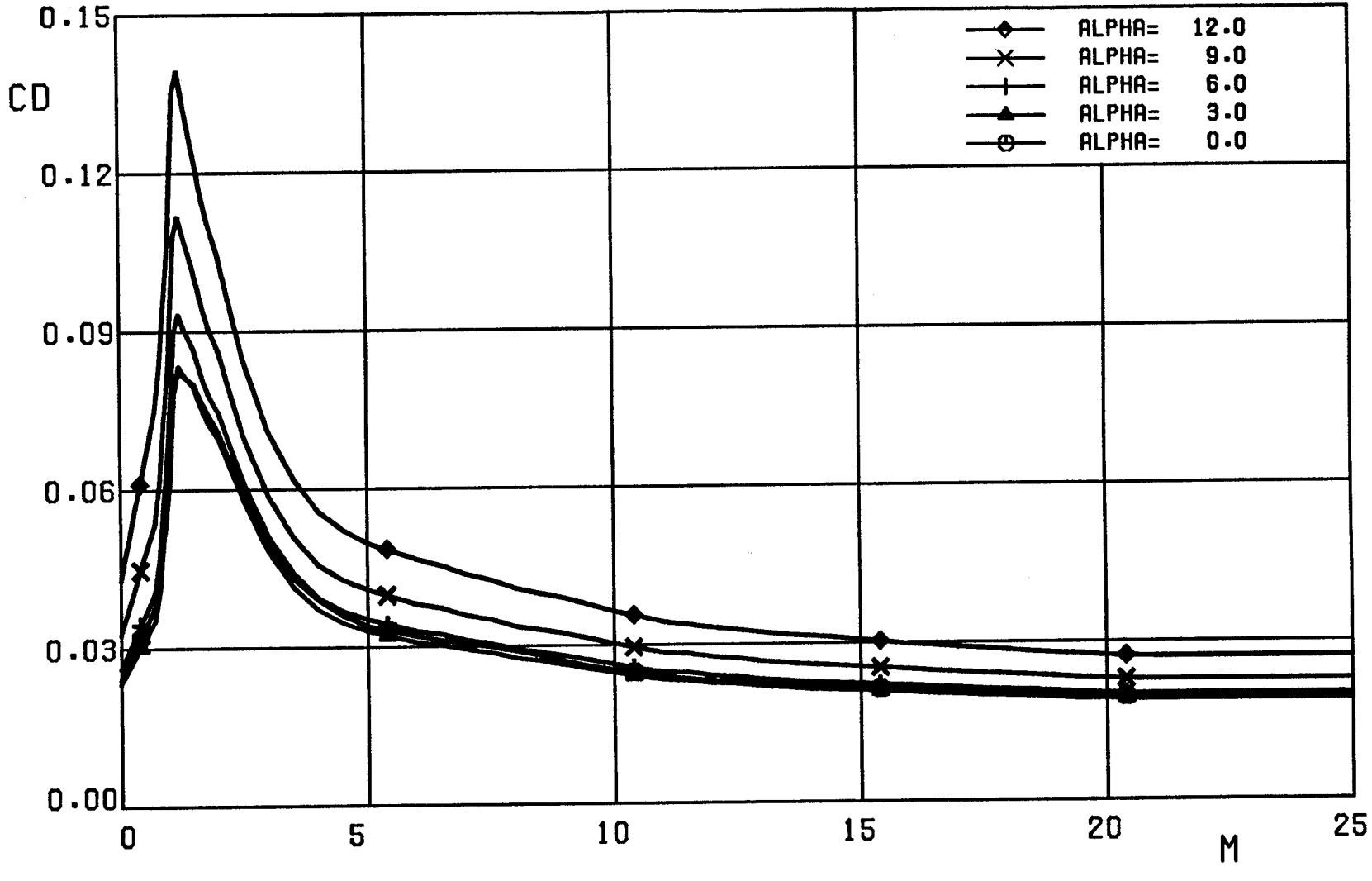

FIG. 1A. DRAG COEFFICIENT,
GHAME CONFIGURATION.

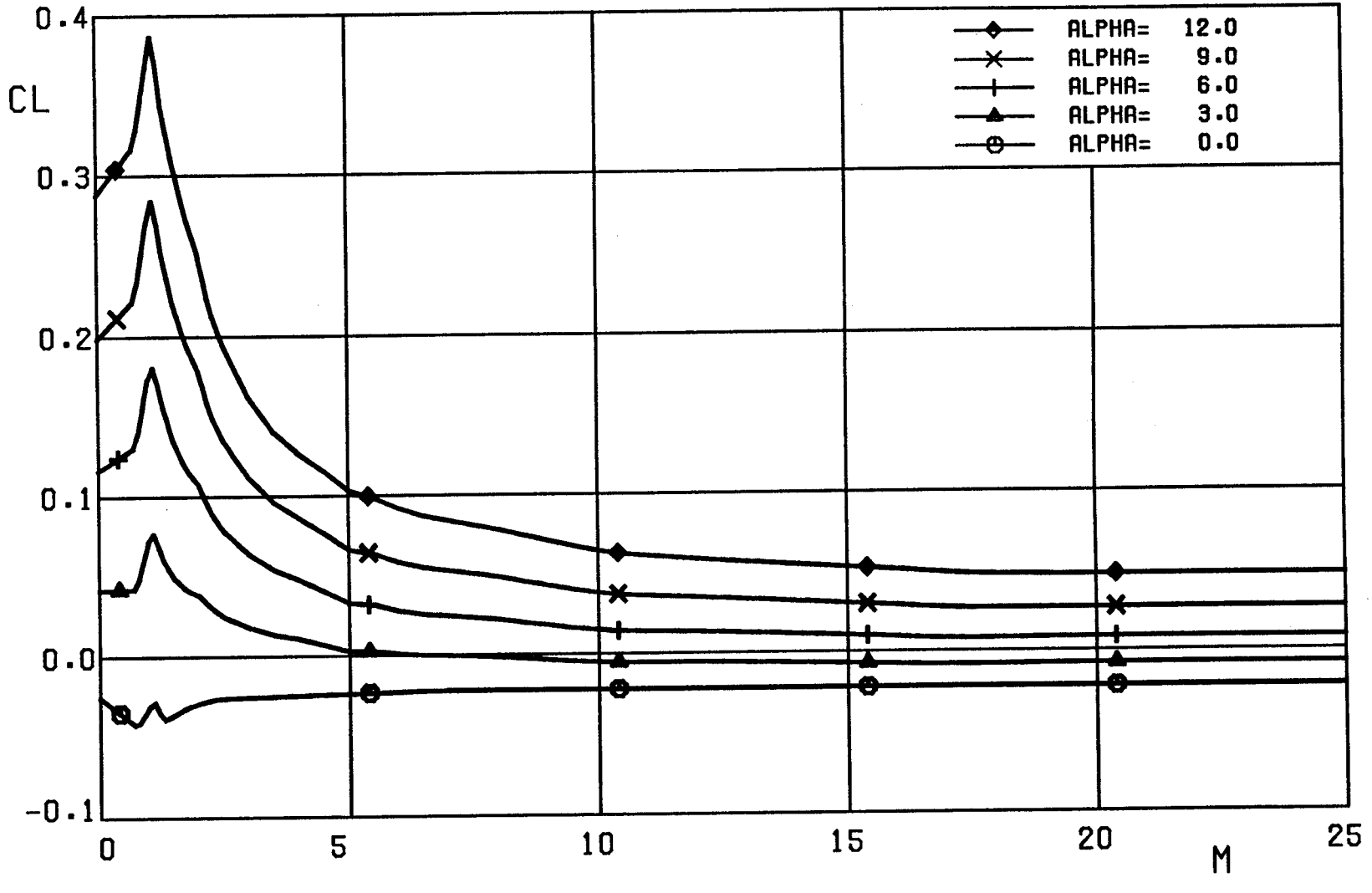

FIG. 1B. LIFT COEFFICIENT,
GHAME CONFIGURATION.

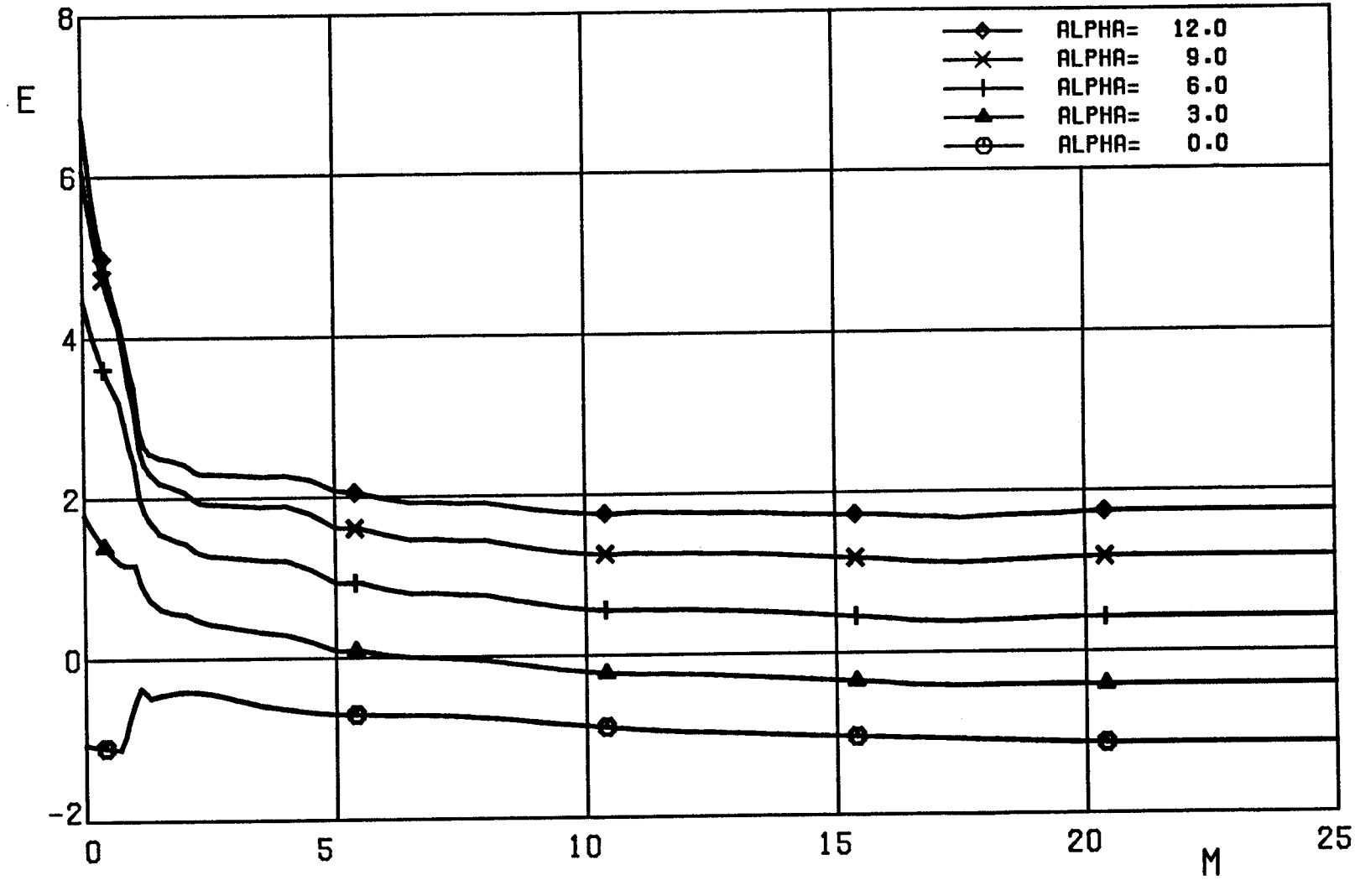

FIG. 1C. LIFT-TO-DRAG RATIO,
GHAME CONFIGURATION.

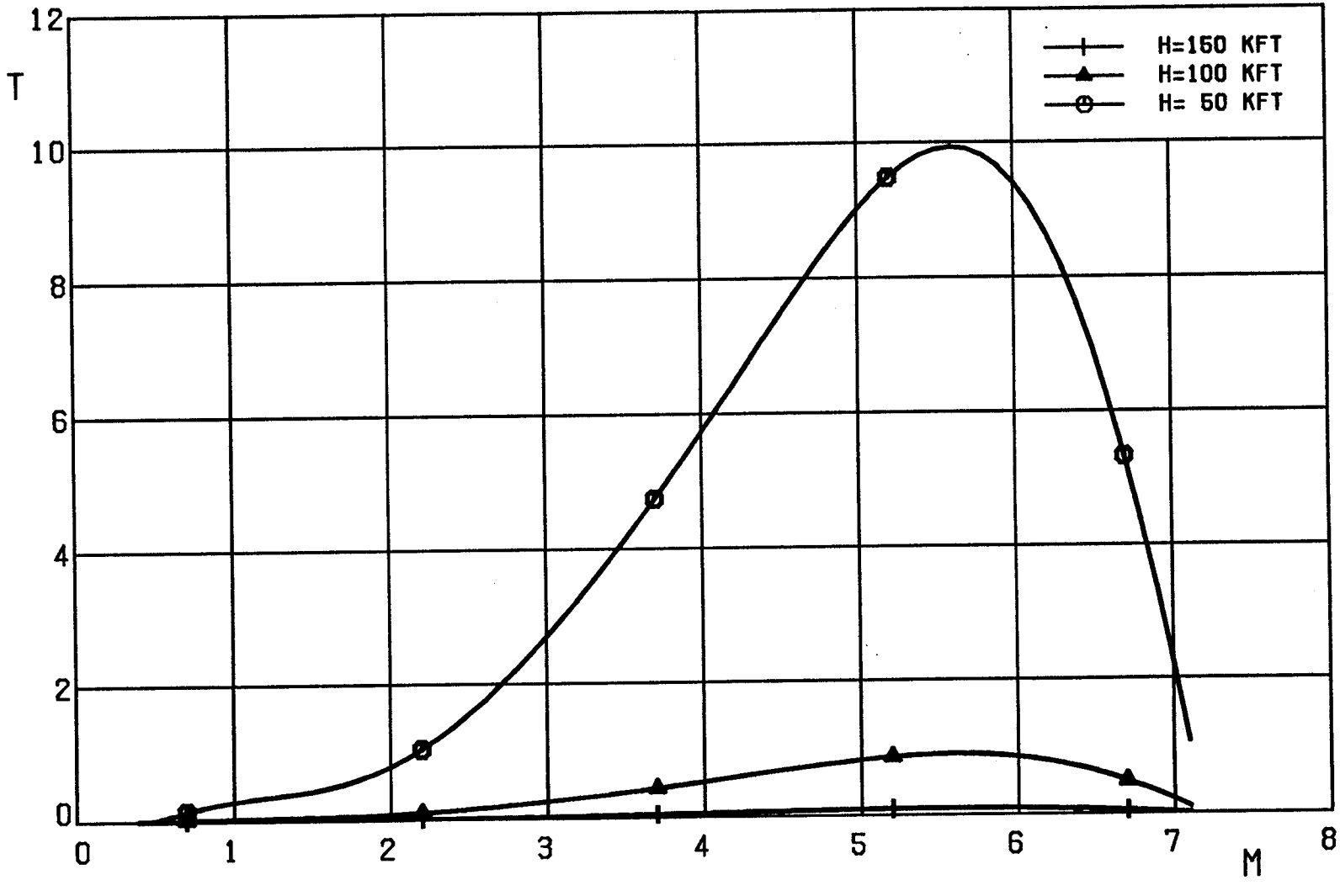

FIG. 2A. THRUST (MLBF), BETA=1, RAMJET ENGINE,
ENGINE MODELS EM1, EM2, EM3.

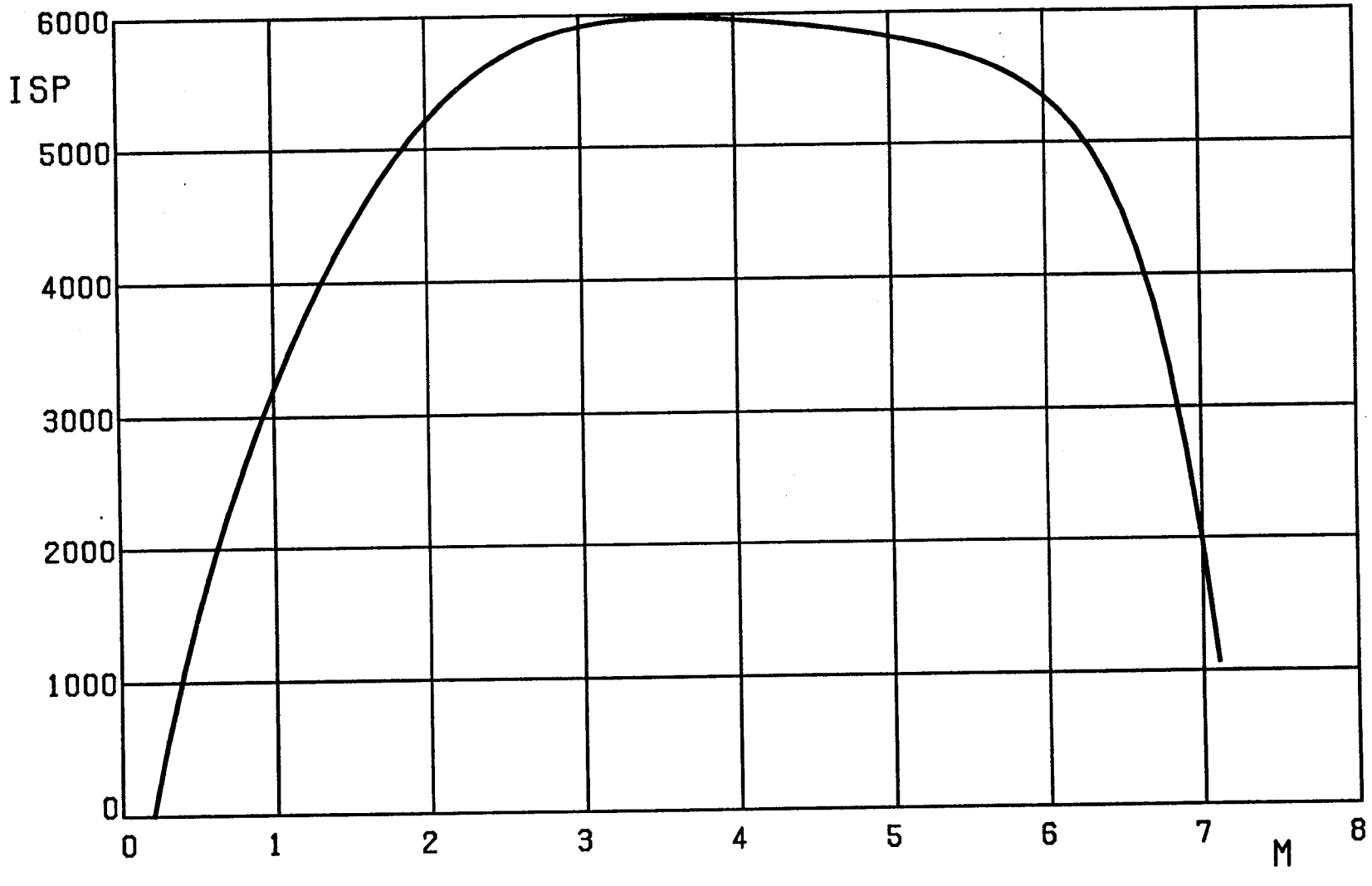

FIG. 2B. SPECIFIC IMPULSE (SEC), BETA=1, RAMJET ENGINE, ENGINE MODELS EM1, EM2, EM3.

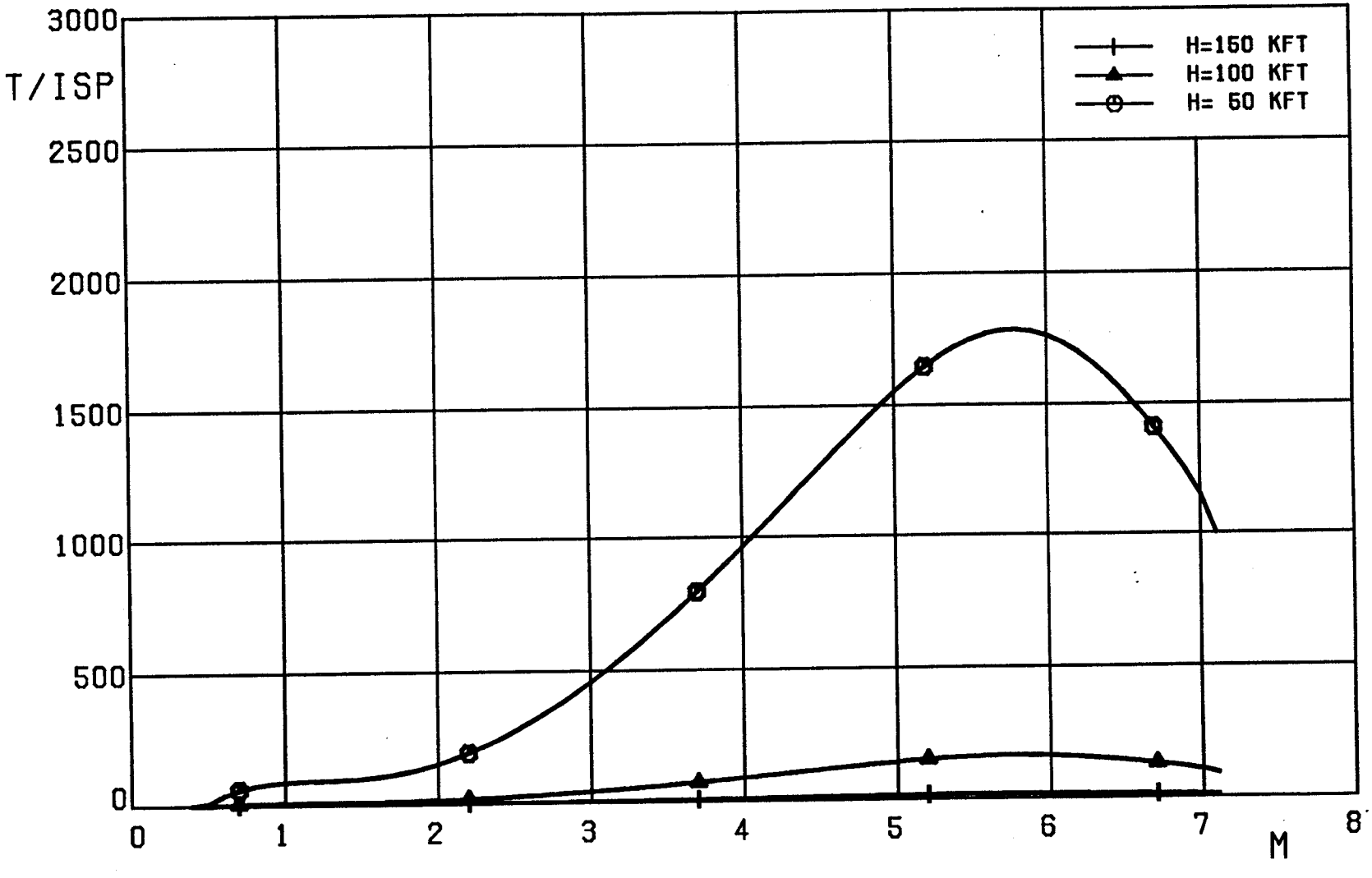

FIG. 2C. FUEL RATE (LBF/SEC), BETA=1, RAMJET ENGINE, ENGINE MODELS EM1, EM2, EM3.

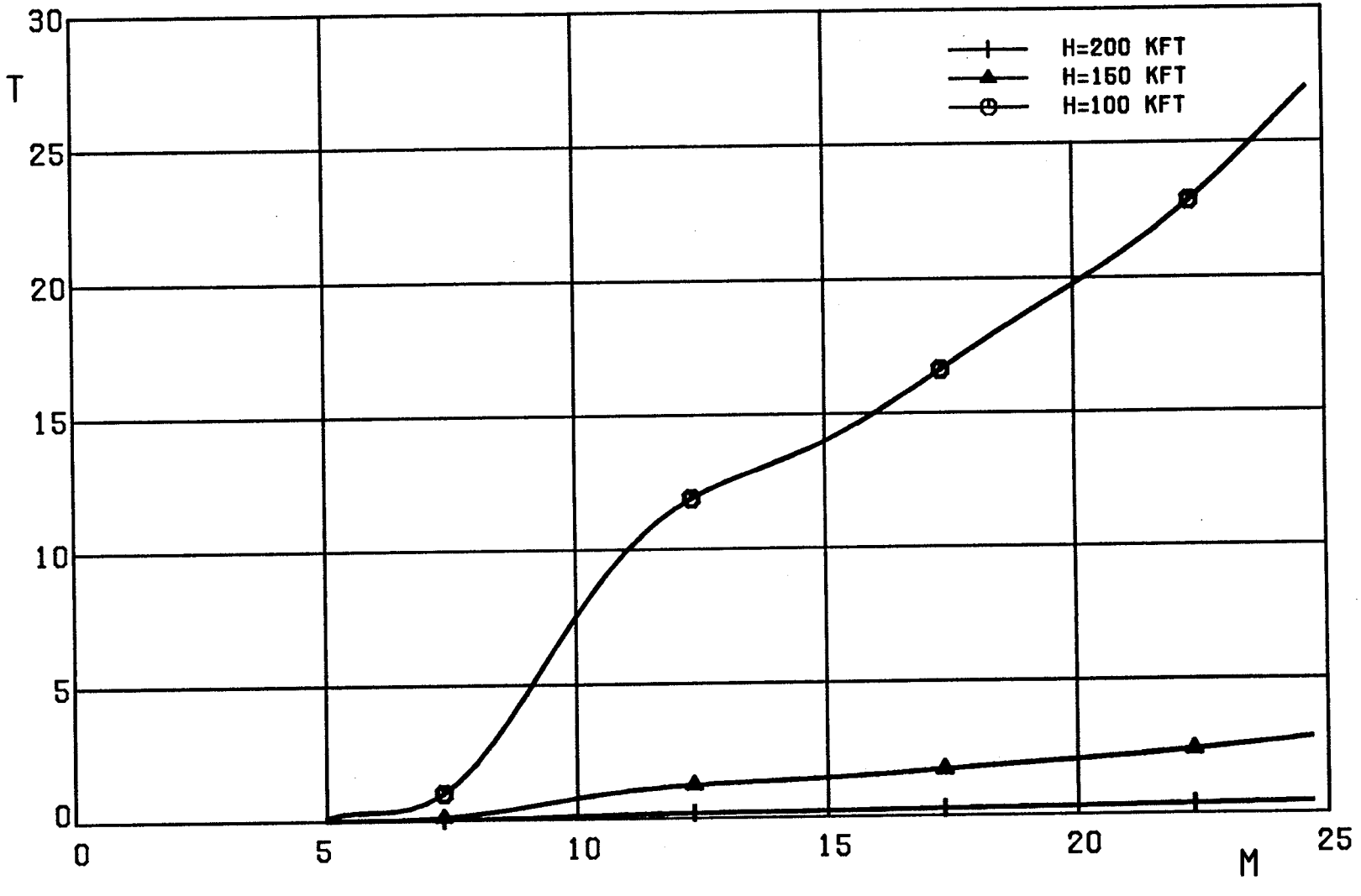

FIG. 3A. THRUST (MLBF), BETA=1, SCRAMJET ENGINE, ENGINE MODEL EM1.

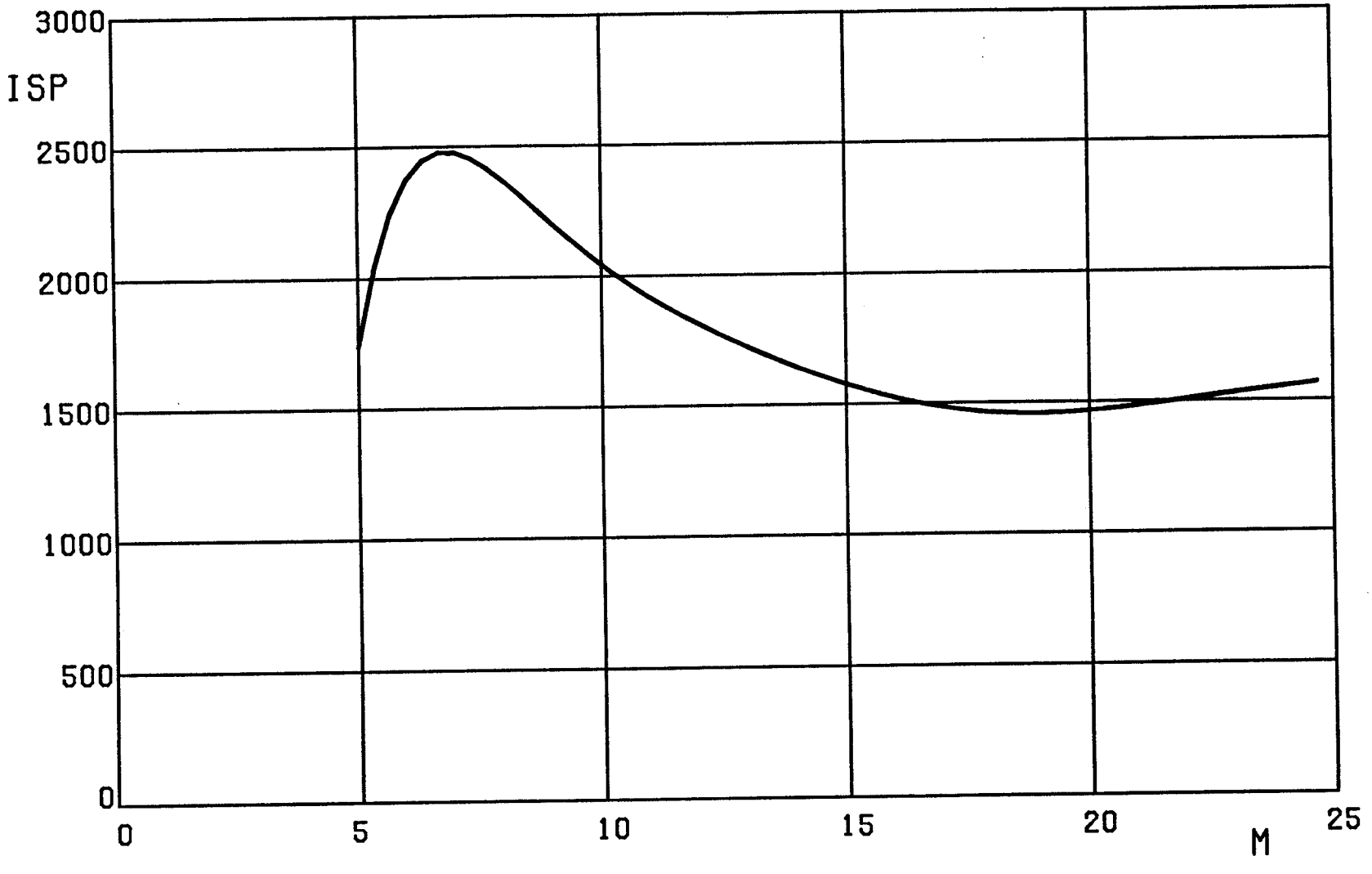

FIG. 3B. SPECIFIC IMPULSE (SEC), BETA=1, SCRAMJET ENGINE, ENGINE MODEL EM1.

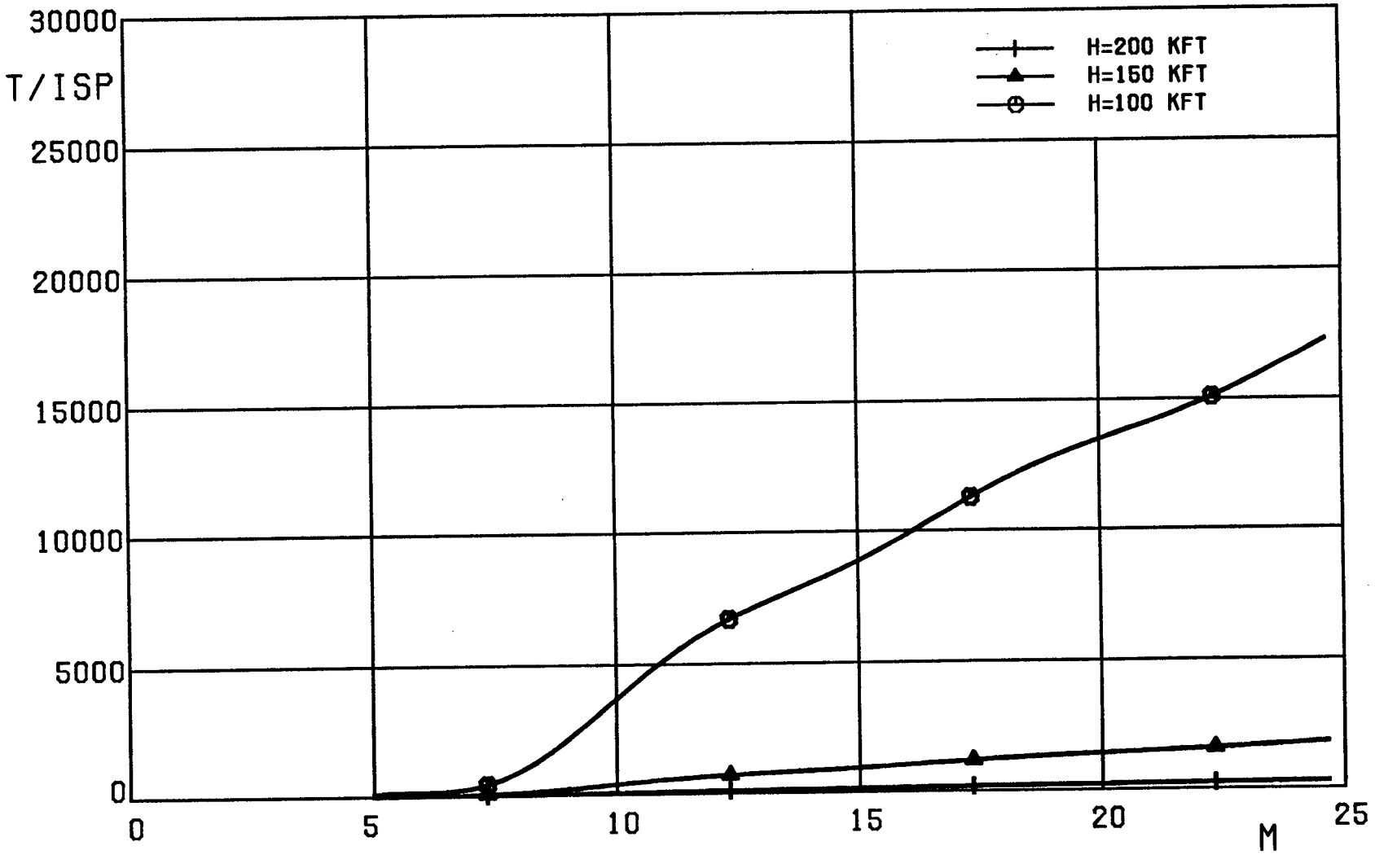

FIG. 3C. FUEL RATE (LBF/SEC), BETA=1, SCRAMJET ENGINE, ENGINE MODEL EM1.

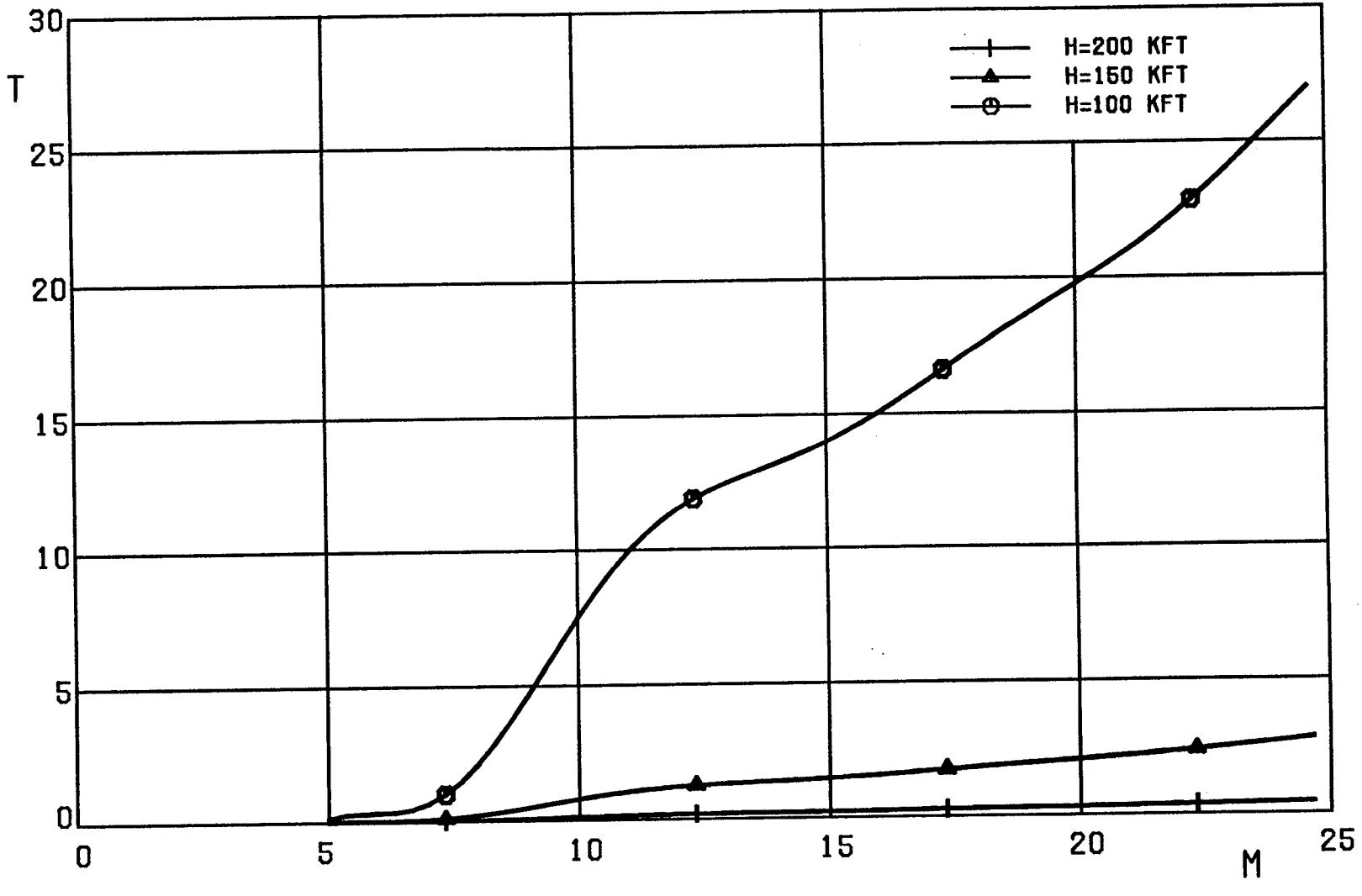

FIG. 4A. THRUST (MLBF), BETA=1, SCRAMJET ENGINE,
ENGINE MODEL EM2.

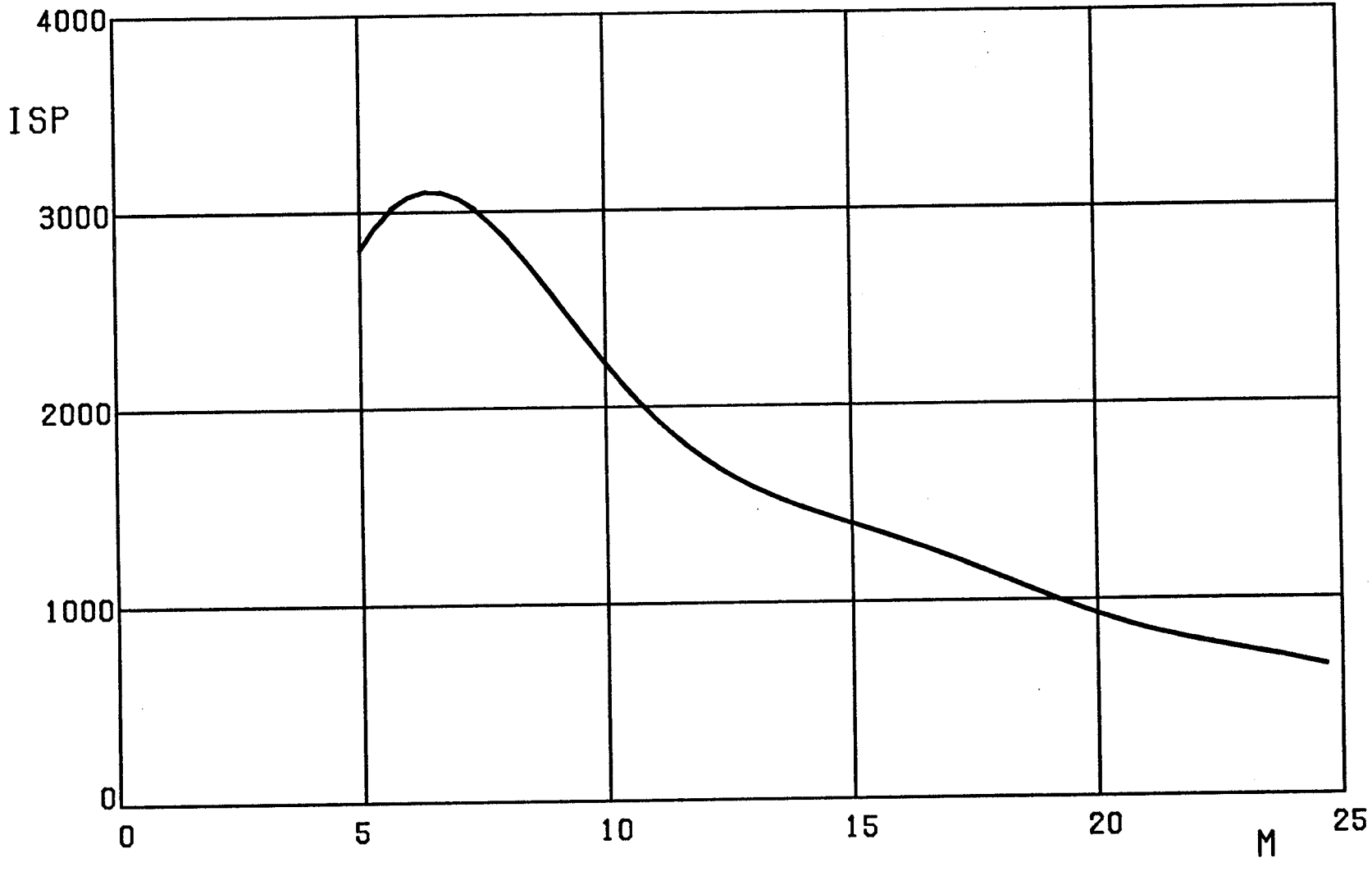

FIG. 4B. SPECIFIC IMPULSE (SEC), BETA=1, SCRAMJET ENGINE, ENGINE MODEL EM2.

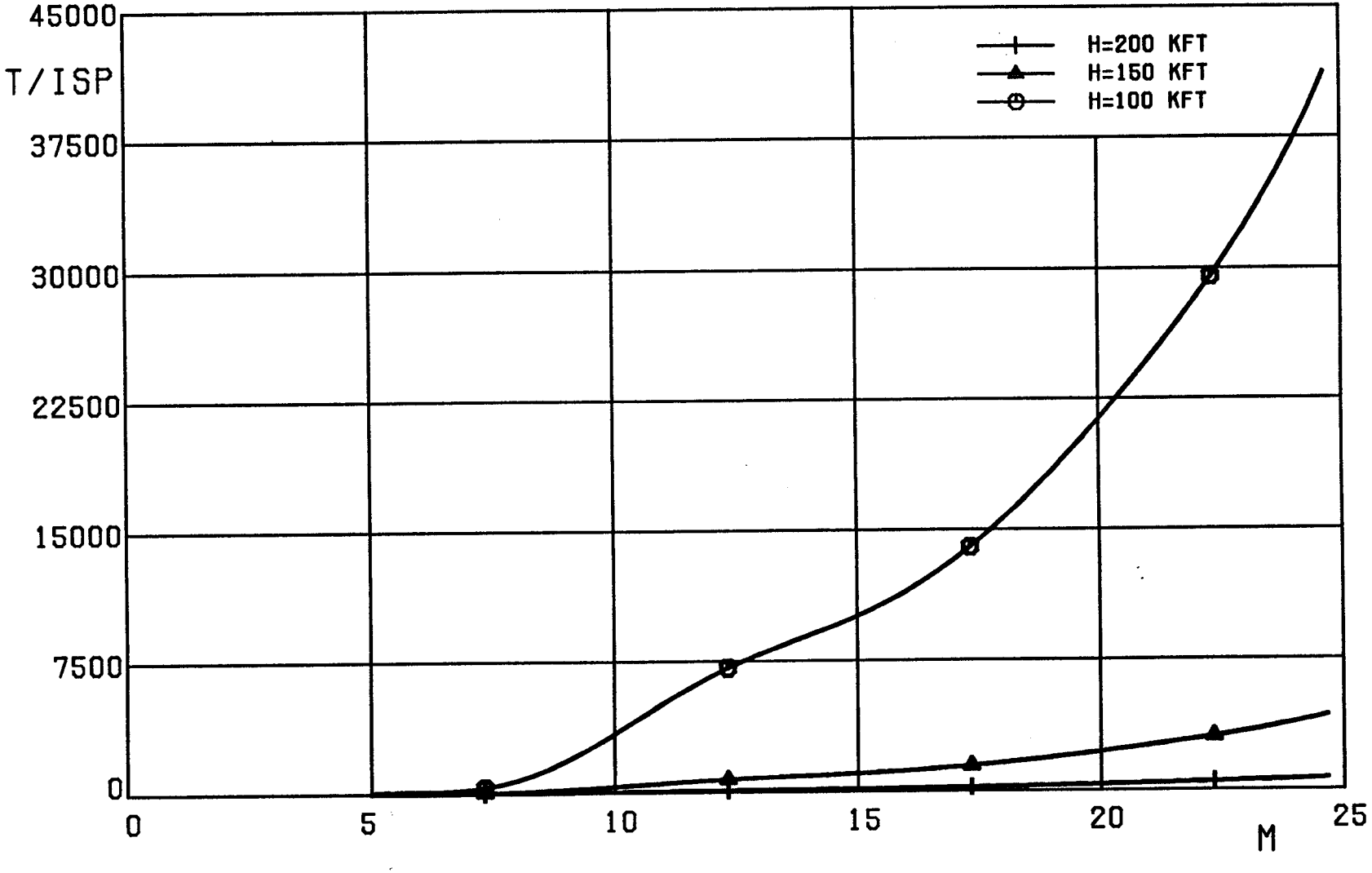

FIG. 4C. FUEL RATE (LBF/SEC), BETA=1, SCRAMJET ENGINE, ENGINE MODEL EM2.

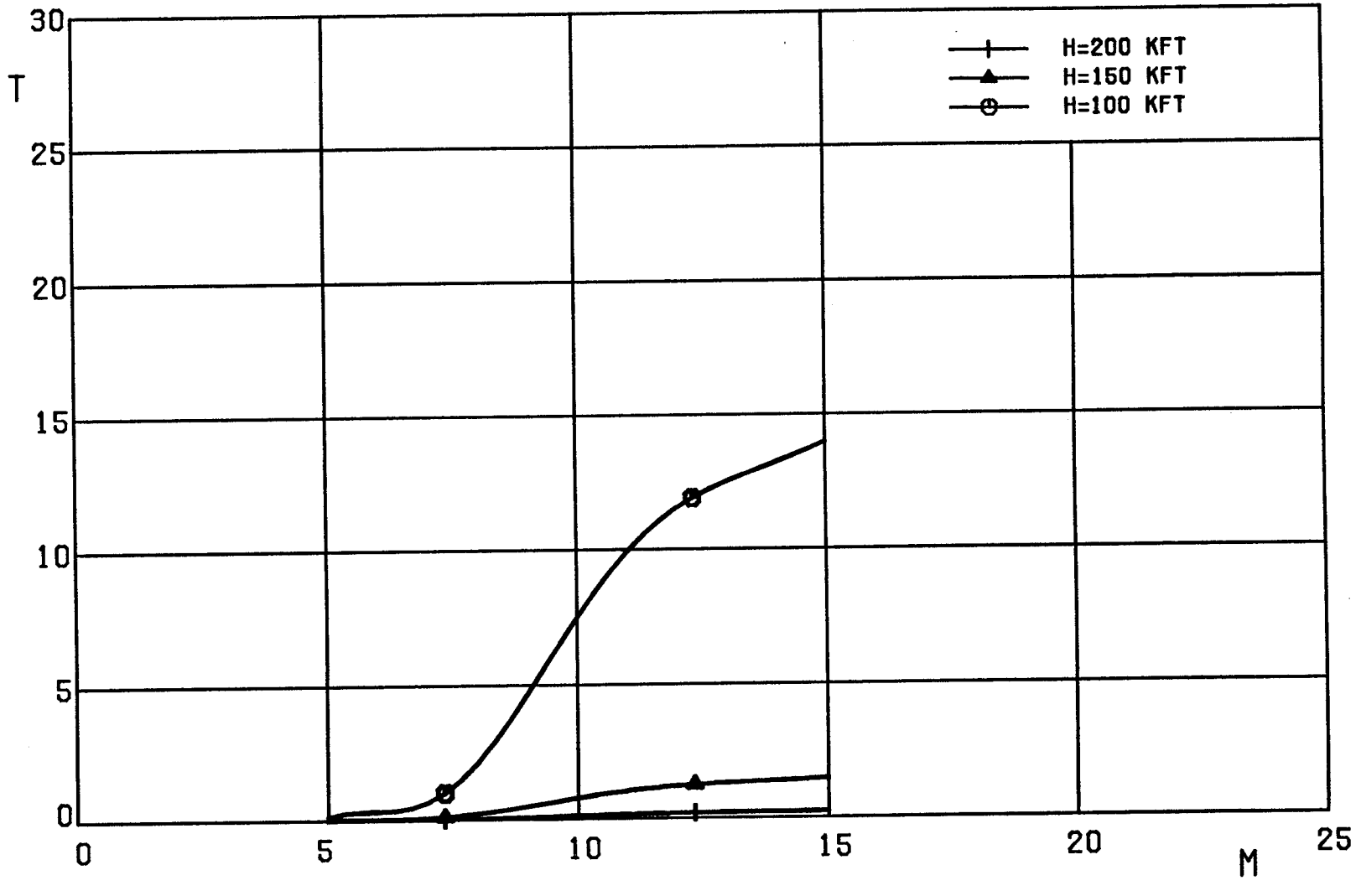

FIG. 5A. THRUST (MLBF), BETA=1, SCRAMJET ENGINE, ENGINE MODEL EM3.

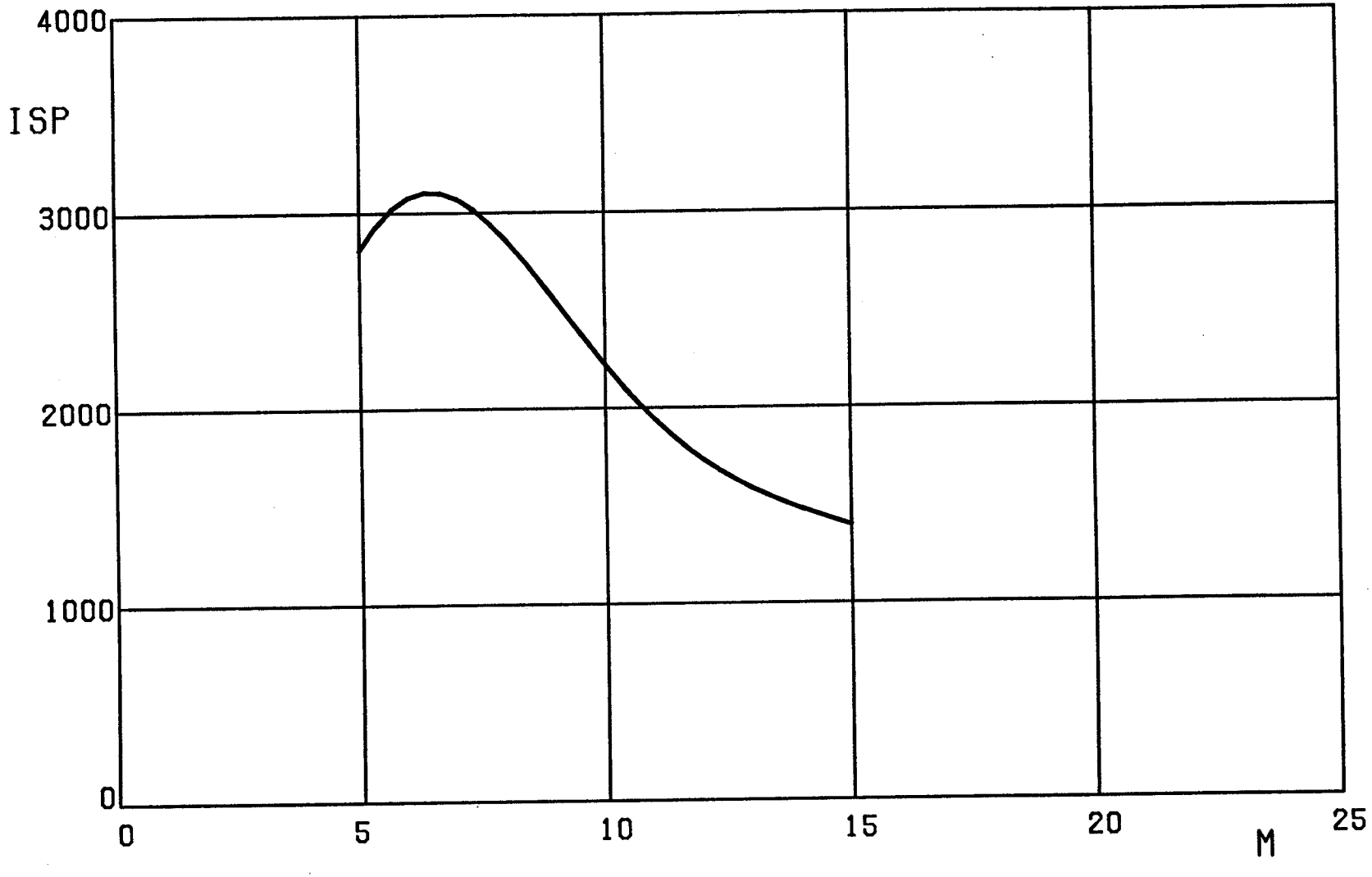

FIG. 5B. SPECIFIC IMPULSE (SEC), BETA=1, SCRAMJET ENGINE, ENGINE MODEL EM3.

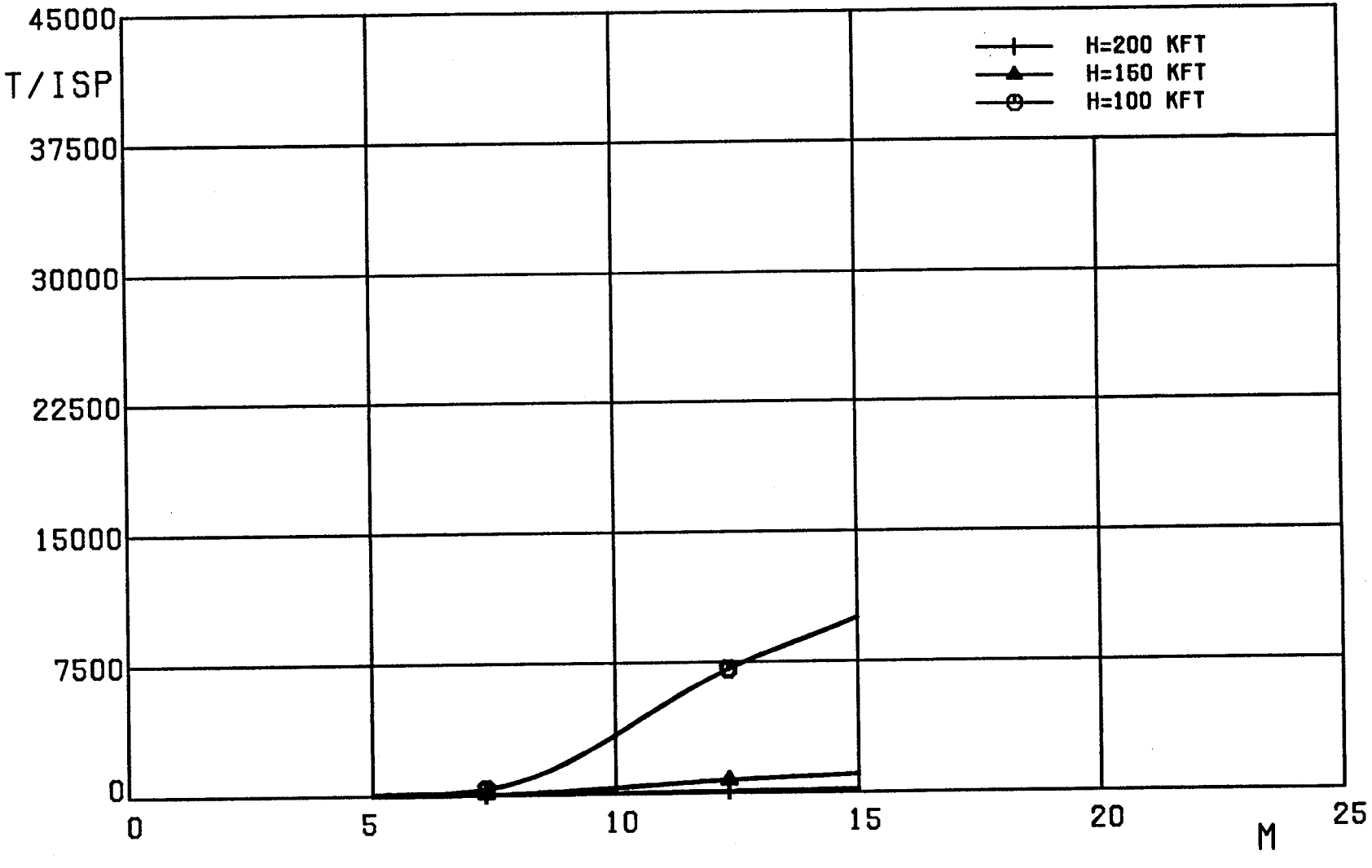

FIG. 5C. FUEL RATE (LBF/SEC), BETA=1, SCRAMJET ENGINE, ENGINE MODEL EM3.

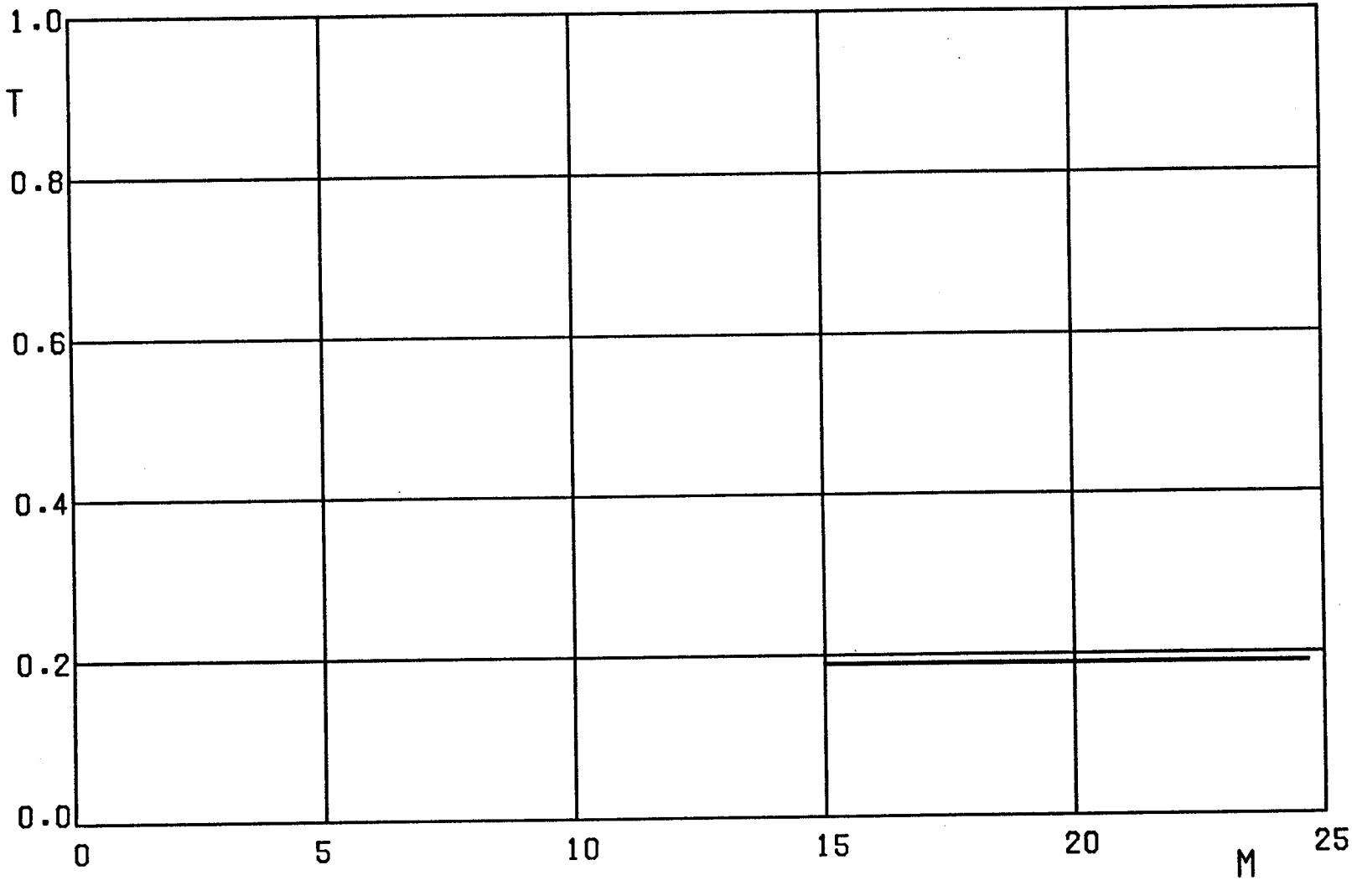

FIG. 6A. THRUST (MLBF), BETA=1, ROCKET ENGINE,
ENGINE MODEL EM3.

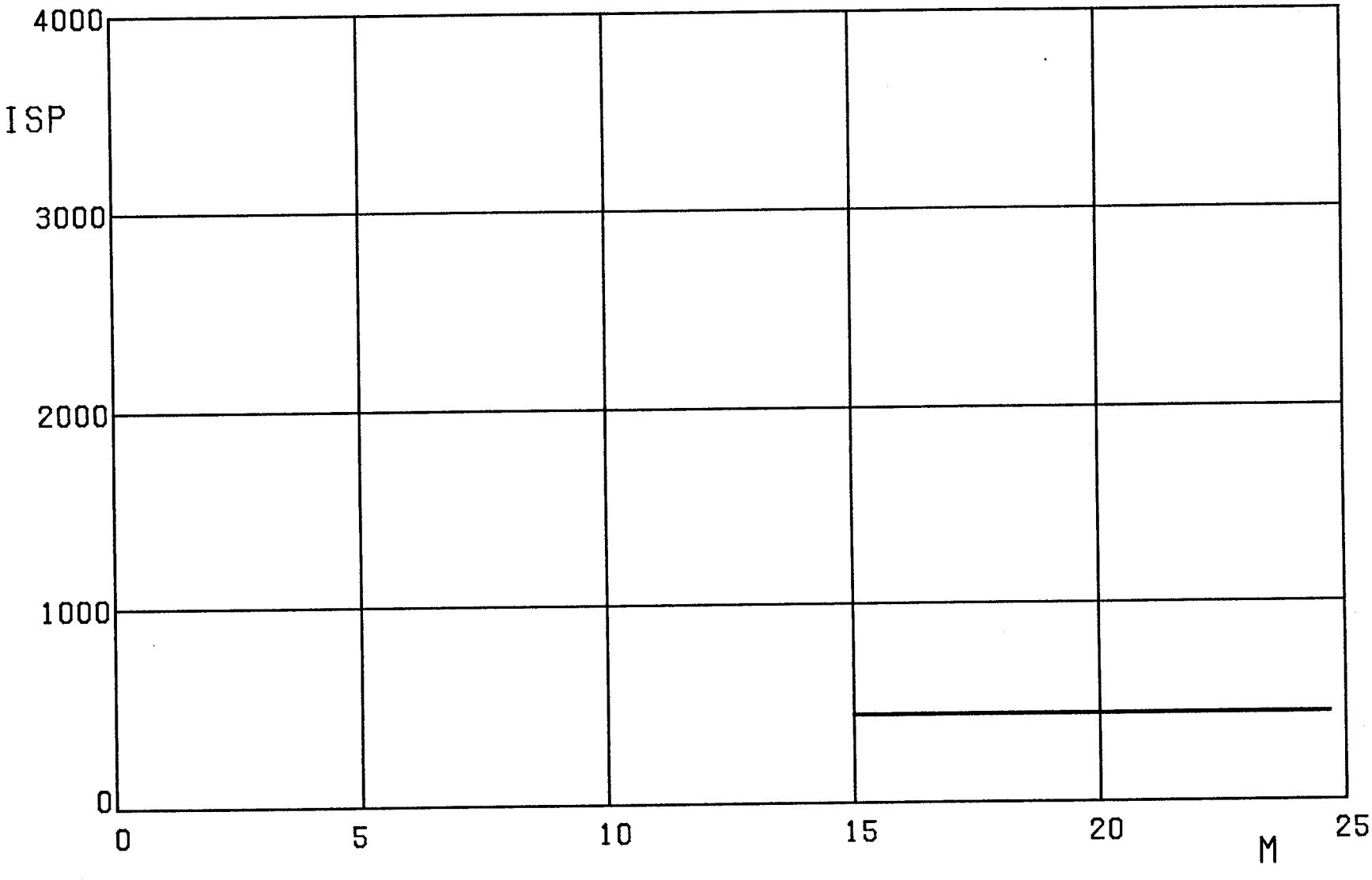

FIG. 6B. SPECIFIC IMPULSE (SEC), BETA=1, ROCKET ENGINE, ENGINE MODEL EM3.

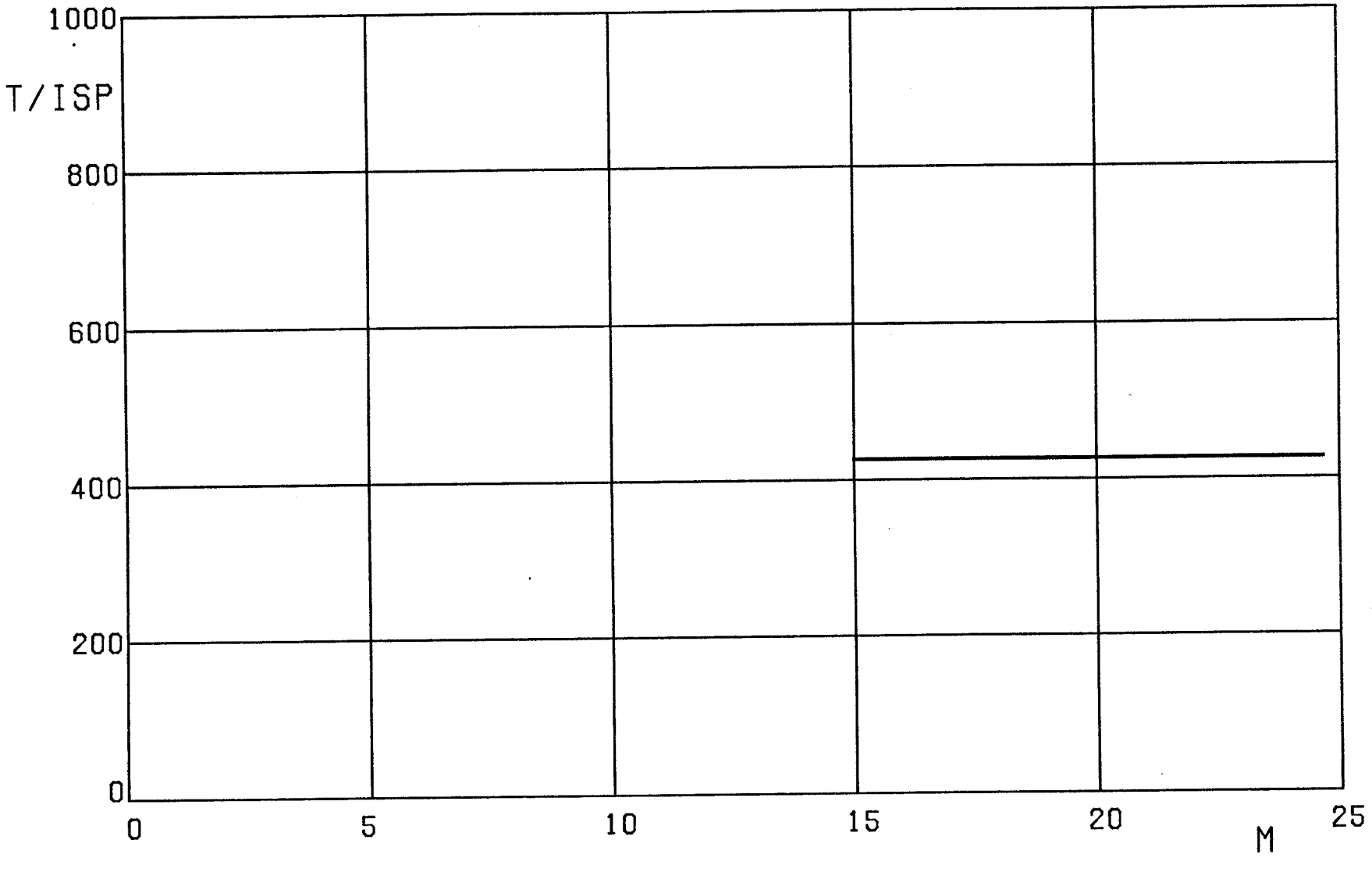

FIG. 6C. FUEL RATE (LBF/SEC), BETA=1, ROCKET ENGINE, ENGINE MODEL EM3.